CHALMERS
UNIVERSITY OF TECHNOLOGY

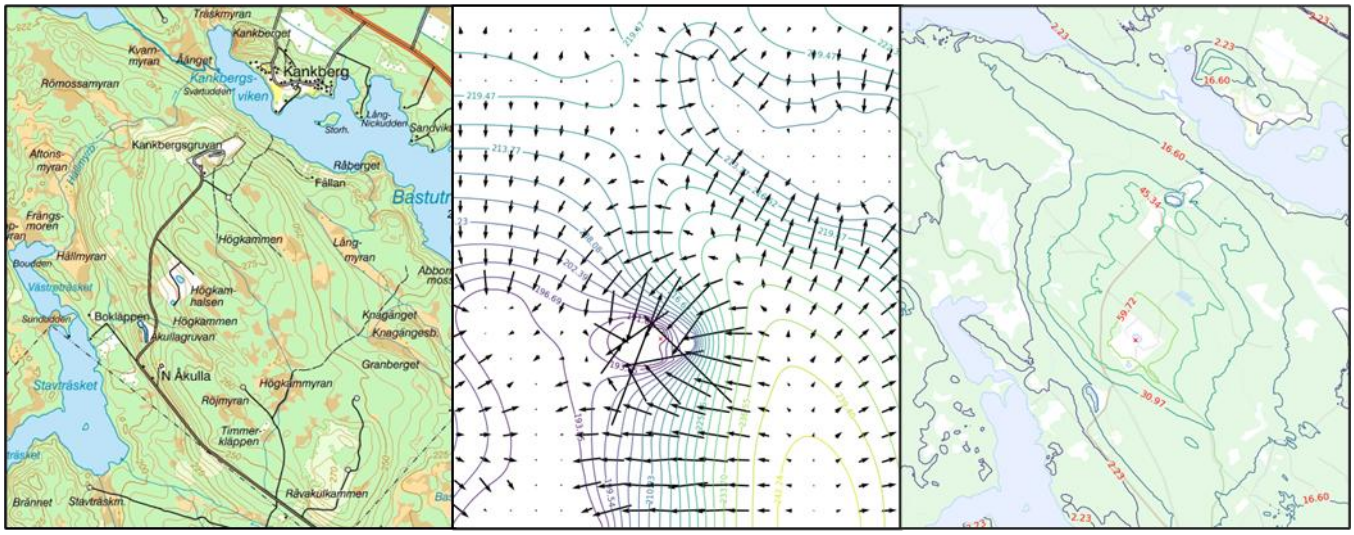

Analysis of Data Value in Numerical Groundwater Modelling at a Mining Site

With Focus on comparison between open-source data model and site-specific data model

Master's thesis in Infrastructure and Environmental Engineering

HASNAIN ALI

DEPARTMENT OF ARCHITECTURE AND CIVIL ENGINEERING
CHALMERS UNIVERSITY OF TECHNOLOGY
Gothenburg, Sweden 2024
www.chalmers.se

MASTER'S THESIS ACEX30

Analysis of Data Value in Numerical Groundwater Modelling at a Mining Site

With Focus on comparison between open-source data model and site-specific data model

Master's Thesis in Infrastructure and Environmental Engineering

HASNAIN ALI

CHALMERS
UNIVERSITY OF TECHNOLOGY

Department of Architecture and Civil Engineering
Division of Geology and Geotechnics
Engineering geology
Chalmers University of Technology
Gothenburg, Sweden 2024

Analysis of Data Value in Numerical Groundwater Modelling at a Mining Site

With Focus on comparison between open-source data model and site-specific data model

Master's Thesis in Infrastructure and Environmental Engineering
HASNAIN ALI

Supervisor: Lars Rosén, professor in the Division of Geology and Geotechnics
David Wladis, Hydrogeologist in Mark & Miljö Hydrosense
Johanna Merisalu, Division of Geology and Geotechnics

Examiner: Lars Rosén, professor in the Division of Geology and Geotechnics

Master's Thesis 2024
Department of Architecture and Civil Engineering
Division of Geology and Geotechnics
Engineering Geology
Chalmers University of Technology
SE-412 96 Gothenburg, Sweden
Telephone: +46 (0)31-772 1000

Cover: Analysis of Data Value in Numerical Groundwater Modelling at a Mining Site

Printed by Chalmers Reproservice
Gothenburg, Sweden 2024

Analysis of Data Value in Numerical Groundwater Modelling at a Mining Site

With Focus on comparison between open-source data model and site-specific data model

HASNAIN ALI
Department of Architecture and Civil Engineering
Chalmers University of Technology

Abstract

Groundwater is a hidden but crucial water source. Studying groundwater flow dynamics is challenging as these systems operate beneath the Earth's surface, surrounded by complexity due to their concealed nature. Understanding groundwater flow is essential for managing water resources and predicting potential contamination risks. This study provides significant insights into the groundwater flow system at the Kankberg mine site. This research aimed to identify a more affordable way to learn about the site than the more costly site testing method. The process involves comparing the hydrogeological results of numerical modeling using open-source data compared to using site-specific data. In this way, assessing the accuracy and dependability of modeling groundwater flow using readily available data will become more feasible. MODFLOW-2005 with NWT solver is selected because of its versatility and acceptance as an industry standard. Two separate data sources were used in the research methodology: open-source data that was readily available to the public and data that was gathered through field investigation. The topographical data and hydrogeological data are collected from the SGU and SLU websites, and the water level of four observation wells is used to calibrate the site-specific model. The water head in different places was manually calibrated to make sure it matched the site's topography. The results show that, compared to the open-source data model, the site-specific data model offered a more accurate simulation. Nonetheless, the open-source data model can still make reasonable predictions and is not all that dissimilar from the field-specific data model. Therefore, for complicated projects with substantial environmental impacts, a balanced approach that combines both open-source data and customized field data can produce more reliable and comprehensive results. This hybrid approach allowed us to evaluate the applicability of these modeling strategies in similar working environments, ultimately leading to better decision-making for environmental management. In conclusion, this comprehensive approach fills a significant gap in understanding the data requirements for numerical modeling in the mining industry. Results from an open-source data model are not too far off from reality. Overall, this research highlights the importance of refining data collection methods and utilizing a combination of data sources for more accurate predictions in the mining sector.

Keywords: value of information analysis, groundwater modeling, numerical model, radius of influence, open-source data, site-specific data, root mean square error.

Acknowledgments

This thesis is the final part of the Master Program Infrastructure and Environmental Engineering at the Department of Architecture and Civil Engineering, Chalmers University of Technology, and was conducted during the spring of 2023 and autumn of 2023. The thesis has been conducted in cooperation with Mark & Miljö Hydrosense and Bergab - Berggeologiska Undersökningar AB. I express my sincere gratitude to my dedicated supervisors, Johanna Merisalu and David Wladis for their unwavering support, guidance, and valuable insights throughout the entirety of this research journey. Special thanks to Lars Rosen for his dual role as both a supervisor and examiner, for introducing me to this fascinating research topic, and for providing invaluable feedback that greatly enhanced the quality of this thesis. I extend my heartfelt appreciation to my friend Maryam for her unwavering support and dedicated time, her friendship is truly valued. Lastly, I want to express my deepest gratitude to my brothers, Ali and Hassan. Without their unwavering support and encouragement, I could not have achieved what I have today. Their constant belief in me has been a driving force, and I am profoundly grateful for the bond we share, which has been an essential pillar of my journey.

HASNAIN ALI
Gothenburg, Sweden, Feb 2024

Table of Contents

List of Figures

List of Tables

1

Introduction

Understanding hydrological processes is essential for scientists and land managers as they investigate the complex relationship between land-use practices and the availability of water resources. In an era marked by climate change, the predictability of the rainy seasons has grown increasingly erratic and vital (Rees et al., 2020). This unpredictability carries significant implications for water resources management, especially considering the growing reliance on subsurface water sources, such as aquifers in rock and unconsolidated deposits, to meet the needs of both human populations and various industrial sectors (Lee and Biggs, 2015).

Groundwater, as a concealed yet dependable water source, serves as a linchpin for water security in many regions. However, unlocking the dynamics of groundwater systems remains a formidable challenge. These systems, operate beneath the Earth's surface and shrouded in complexity, making them elusive subjects of study. This is where groundwater modeling emerges as an indispensable tool, offering a comprehensive approach to analyze, forecast, and manage these clandestine water resources. By employing advanced techniques, groundwater modeling empowers decision-makers to make informed choices regarding subsurface water resources, shedding light on their behavior and distribution (Sun et al., 2011).

However, it is necessary to consider the limitations of this modeling technique. Despite their great value, groundwater models typically struggle to incorporate the necessary measurement scale with time and budget constraints. As such, they may not always offer precise predictions of groundwater flow in real-world scenarios (Delottier, 2016). Several data sets can be gathered to improve the calibration process and qualitative trends in the results can be examined to address the problem. By implementing these practices, decision-makers can effectively address uncertainties and complexities in the decision-making process (Delottier, 2016). Additionally, a robust grasp of the modeling techniques is essential for model conceptualization and reducing result uncertainties, as highlighted by Praveena et al., (2010).

In this context, it is essential to develop a system that can effectively adapt to these changing conditions and ensure the sustainable use of water. Such a system should incorporate advanced techniques capable of accurately predicting water inflow from different sources for the designated area, thereby optimizing water allocation strategies. Furthermore, it should harness the power of machine learning algorithms to continually enhance the precision of available site specifications and groundwater data to optimize the sustainable use of water allocation schemes.

This thesis, focused on Kankberg Mine, located in the Västerbotten Region in north Sweden, intends to contribute to a thorough understanding of water resource dynamics and to provide creative solutions for resilient water management techniques. The numerical modelling

method is used to analyse the geology and hydrogeology of this site by considering steady conditions for a long time. In the mining industry, it is common to find ore deposits below the water table. This presents a challenge since groundwater seeps into these areas, resulting in flooding and disturbances to mining activities. To create a dry and safe working environment for miners, a large amount of excessive groundwater is pumped out, which causes the depletion of local water sources. Apart from that, a lot of water is used for mineral processing such as ore crushing and grinding, and even more water is needed to make slurry to transport processed minerals like coal through a pipeline network (Xiao-jun, 2012).

Furthermore, open-pit mines and drilling processes generate a large amount of dust particles, which can lead to air pollution and respiratory issues for both miners and nearby communities. To handle this problem, companies use plenty of water to spray on dust particles to reduce their impact on the environment (Panigrahy et al., 2015). This excessive use of water in mining operations not only depletes local water sources but also puts a strain on the overall water supply in the region. These effects can lead to the drying up of wells and springs, impacting local communities that rely on groundwater for drinking water and irrigation (Li, Cohen, and Zhang, 2018). As a result, proper management and monitoring of groundwater levels are necessary to ensure sustainable mining practices and avoid any negative effects on the surrounding ecosystems. This helps to preserve precious freshwater resources and reduce the environmental impact of mining operations. Therefore, it is crucial to ensure that mining operations do not contaminate groundwater sources.

Additionally, excessive groundwater extraction can also in certain areas cause land subsidence, damage infrastructure and increase the risk of sinkholes (Feng et al., 2008). Furthermore, the depletion also has ecological consequences, as it leads to the loss of habitats for various species (Wanner et al., 2019). This can result in a loss in biodiversity and negatively impact the overall health of the ecosystem, affecting plant and animal species that rely on these habitats (Wanner, P., 2019). These issues emphasize the importance of using sustainable groundwater management techniques in the mining industry and impact nearby communities that rely on these water sources for their livelihoods.

1.1 Motivation

When gathering hydrogeological data in the field to build groundwater models, several problems may arise. Initially, fieldwork can be physically challenging due to lack of infrastructure on-site and limited access to equipment and resources in remote locations. Rough topography, rolling hills and dense vegetation can make this job more stressful. Moreover, the presence of sensitive ecosystems or protected areas may require extra precautions and careful planning to minimize environmental impact during field investigations for groundwater modeling. Working near an active mine exposes the crew to potential danger and raises health and safety concerns. Afterward, further environmental permits can be needed based on how sensitive the area is to drilling and sampling. Conducting groundwater modeling in densely populated areas may require additional precautions, such as the involvement of local authorities and stakeholders to mitigate

potential disturbances. Due to the cold temperatures, many mining sites in northern Sweden face extremely difficult weather conditions that make fieldwork slow and difficult to conduct. These circumstances may cause the project to run behind schedule and go over budget. Investigation of large area require extensive data collection and analysis, which can be time consuming and resource intensive. The use of advanced technology and equipment requires skilled workers, making these operations complex and costly to execute. Breakdown of drilling and sampling equipment, hiring additional crews for unanticipated issues, permissions to access private properties for boreholes, and placing infrastructure introduce additional logistical challenges. Table 1-1 describes the key reasoning behind the choice of groundwater modeling.

Table 1-1. Motivation behind the selecting groundwater technique.

		Open-source Data Model	Site-specific Data Model
1.	Time, cost, and work environment in gathering hydrogeological data.	✓	✗
2.	Environmental permits for drilling and sampling.	✓	✗
3.	Exposes the crew to potential danger and raises health and safety concerns.	✓	✗
4.	Advanced technology and equipment require skilled workers.	✓	✗
5.	Quality and quantity of data.	✗	✓
6.	Degree of uncertainty.	✗	✓
7.	Degree of validity of conceptualization.	✗	✓

On the other end of the spectrum, the quality and quantity of data gathered during field tests have a big impact on numerical groundwater modeling. Having adequate data on site geology, groundwater levels, and flow rates makes it easier to calibrate and accurately simulate the behaviour of the aquifer system. It also reduces the degree of uncertainty in the entire model. Furthermore, the conceptualization of this type of model has a high degree of validity since it captures the true complexity and diversity of hydrogeological systems that exist in reality.

When there are gaps in the time frame and geographical data, it raises concerns about the reliability of results and future prediction in the model. Therefore, ensuring a sufficient amount of reliable data is collected during field tests is essential for producing reliable groundwater models.

Long-term monitoring provides a wide range of calibration and validation data points that allow results to be carefully checked against independent observations, enhancing confidence in the predicted outputs for future scenarios. Frequently collecting data includes tracking dewatering, recharge flow rate, and other geological changes over time in response to mining activities.

Numerical modeling is an effective tool for predicting the impact on groundwater conditions from a mining operation; however, modeling can be made on different levels of detail regarding both the model setup and the data used for the modeling. Detailed modeling can be very costly and complex but such detailed modeling may not always be motivated to solve a specific problem. There is a need to understand what level of detail in the model setup and what amount of information is required to get a model result that is good enough for the particular problem at hand.

1.2 Aims and Objectives

The aim of this study is to evaluate the potential benefits of acquiring new information and determine whether it is worthwhile to spend the time and money obtaining it. The following are the required objectives of this analysis:

1. What is the value of more data in a numerical groundwater model?
2. Can a numerical model with open data get similar results as numerical modeling with data from site-specific pumping tests?
3. Investigating the accuracy of the numerical model depending on the data type.

1.3 Limitations

There are some important limitations while doing numerical modeling for these sites.

1. A single site is considered. To increase the validity of the results and conclusions, it would be worthwhile if similar work could be done in other locations.
2. MODFLOW was chosen as the model because of its versatility and acceptance as an industry standard. Although other numerical models are better suited to take fractured rock properties into account, these models cannot be investigated for this project due to time constraints.
3. Due to the limited resources, information from Hydrosense and Bergab consultancies was the only site-specific data used to assess the information's value.

1.4 Thesis Outline

This outline has been thoughtfully designed to provide a clear and logical breakdown of the study. This thesis is organized into five distinct sections to provide a clear understanding of this research, in addition to this introductory chapter. The second section (Chapter 2) comprises a theoretical background where the foundational theories behind groundwater flow are explained. This section also provides a concise overview of the applied methodologies. Chapter 3 examines deeper into the specific aspects of setting up the models, followed by the

catchment area and its hydrogeology. Furthermore, it contains an in-depth presentation of the chosen case study site, the Kankberg Mine.

Moving forward to the fourth section (Chapter 4), which defines the methodology employed throughout this study and offers a comprehensive insight into the general approach adopted. The numerical results from the models are presented in the subsequent chapter (Chapter 5), and the qualitative viewpoints of groundwater regarding open data are also included in this section. Finally, Chapter 6 focuses on a thorough analysis of the model conclusion and compares it to the results of related studies in the area.

2

Theoretical Background

This chapter provides the theoretical underpinnings for some of the main concepts that are used in this study namely, groundwater principles, water protection areas (WPAs), modeling, numerical models, analytic element models (AEMs), uncertainty, and Monte Carlo Simulation (MCS).

2.1 Source of Inflow

Studying groundwater is crucial as it helps us understand its quality, quantity, and movement patterns. The functionality of underground water reserves in a particular area is quite distinct and it heavily depends on its sources. The most vital sources are rainfall, rivers, and even melting snow (Maulé, Chanasyk, and Muehlenbachs, 1994). Additional sources of water include water used for irrigation, seepage from lawns, septic systems, drinking water distribution networks, and even from factories. In arid regions, water is artificially added to the ground during dry seasons when rainfall is insufficient to meet the water demand (Igboekwe and Ruth, 2011).

Additionally, the geographical features of the area, such as the presence of permeable rocks or soil, can also play a significant role in the functionality of these reserves (Zarate et al., 2021). To study the recharge process of a groundwater reservoir, experts use wells and monitoring equipment. By analyzing the data collected from wells and equipment, experts can make informed decisions regarding the sustainable management of underground water reserves (Hssaisoune et al., 2017). Furthermore, this knowledge allows us to identify potential risks such as contamination or depletion, ensuring the long-term availability of this valuable resource (Hssaisoune et al., 2017).

2.2 Groundwater Recharge

Groundwater recharge occurs through the natural movement of water from the land surface into underground aquifers. Depending among many other things, some of the precipitation that falls as rain or melts as snow evaporates into the air, some run off onto the land surface, some water absorbed by plants evaporate through transpiration into the air and the remaining water infiltrates into the soil or rock, where it starts to percolate downward (Bhanja et al., 2018). These processes of infiltration and percolation allow water to enter the soil or cracks within bedrock due to the force of gravity or negative pressure (Vadose zone). The rate at which water penetrates into soil mainly depends on factors like porosity, hydraulic gradient, and the slope and texture of the land surface, among others (Zecharias and Brutsaert,1988).

2.3 Groundwater Flow

Hydrologists employ a variety of mathematical techniques to calculate the rate of groundwater recharge. The water balance technique which is shown in Equation 2-1 is one approach that measures recharge as the water that remains after subtracting runoff and evaporation from the total precipitation that occurs in a catchment area (Sutcliffe, 2004).

$$\Delta S = P - ET - R \qquad \text{Equation 2-1}$$

Where:

P = Precipitation
ET = Evapotranspiration
R = Runoff
ΔS = Change in soil water storage

Based on characteristics like hydraulic conductivity and water potential differences, Darcy's law which is shown in Equation 2-2, can also be used to measure the vertical subsurface flow through Unconsolidated deposits and rock layers. Darcy's law is typically useful in estimating groundwater recharge in a saturated zone where water flows naturally. By combining the water balance technique with Darcy's law, Hydrogeologists can obtain a more comprehensive understanding of groundwater recharge rates and patterns (Fetter, 2014).

$$Q = -\mathrm{KA}\,\frac{\Delta h}{\Delta l} \qquad \text{Equation 2-2}$$

Where:

Q = Total discharge or volume flowrate
A = Cross-sectional area
K = Hydraulic conductivity, K is a function of the water content in the geologic medium
$\frac{\Delta h}{\Delta l}$ = Hydraulic gradient

Furthermore, researchers have developed hybrid models by combining empirical equations and numerical models to calculate the occurrence of rain due to climate change and groundwater recharge. This technique is cost-effective and less time-consuming (Goodarzi et al., 2015). Each technique has its own advantages based on the available information and the level of precision needed for the recharge measurement.

2.4 Groundwater Modeling

A model is intended to help us understand and predict how complex systems will work in the real world. This technique can be used in many fields, not only engineering and science, but it can also simulate economic and even social science situations as well (Anderson et al.,

2015). The conceptual model is a description of the flow system that must be simplified in order to build a model with the necessary complexity to solve the issue. Based on accessible field data, it can be displayed as text, tables, charts, and diagrams. A more effective model is one in which subsurface head conditions are presented in space and time. In general, there are two types of groundwater models: physical (laboratory) models and mathematical models (Anderson et al., 2015). Mathematical models utilize equations to depict and simulate groundwater movement, while physical models involve the construction of physical replicas.

Physical models are useful for understanding the behaviour of groundwater in controlled laboratory settings. However, they may not accurately represent the complex and dynamic nature of real-world hydrogeological systems (Anderson et al., 2015). On the other hand, mathematical models can incorporate various parameters and boundary conditions to simulate groundwater flow in a more realistic manner (Anderson et al., 2015). These models can provide valuable insights into the movement and distribution of groundwater over time and space, aiding in decision-making processes related to water resource management and environmental planning.

Mathematical models can be either data-driven or process-based. Data-driven models, also known as statistical models, work with large amounts of observational data to find dependencies and relationships that allow the prediction of values for unknown variables. Modern machine learning techniques have led to a significant evolution of these kinds of models, making them more predictive. In contrast, process-based models apply physical principles to represent groundwater flow within a specific area and they can be predictable or unpredictable.

2.4.1 Conceptual Model

Conceptualization is a crucial step in the modeling process as it involves identifying and defining the key components, relationships, and processes that need to be represented in the model. This step helps to ensure that the model accurately represents the real-world scenario and can be used to make reliable predictions or decisions. Additionally, conceptualization also helps in identifying data requirements and potential limitations of the model.

It can be generic but is usually built according to a specific site hydrogeology (Winter, 2001). Inaccurate conceptualization often leads to poor model calibration (Anderson et al., 2015). However, it is important to note that the accuracy of the conceptual model heavily relies on the availability and quality of data. In general, inadequate data can increase limitations in the numerical model's predictions as well as increase uncertainty. Furthermore, it is crucial to consider the spatial scale of the model, as it can also affect its accuracy in real-world scenarios. The purpose of the modeling determines the amount of information needed in the conceptual model. Adding too much complexity to the initial stage of conceptualization could make it difficult to interpret and analyze. Additional data can be included later on in the modeling process, if necessary.

2.5 Numerical Model

Numerical modeling is the process of simulating natural systems and issues using quantitative techniques like arithmetic. Most of numerical model applies mathematical equations that explain the subsurface movement of water via porous material to groundwater systems (Fetter, 2014). Numerical techniques and computer programs are used to discretize and solve these equations, which are based on the concepts of fluid mechanics. Darcy's law is one of the fundamental mathematical equations that serves as a foundation for understanding how water moves through porous materials. It describes the flow rate of groundwater according to the hydraulic gradient, hydraulic conductivity, and area of the porous material. Darcy's law is applied under the premise that water is flowing through a saturated medium with a content flow density. The final form of the water balance equation that describes the flow through a porous medium, is presented in Equation 2-3, as sourced from Anderson et al. (2015).

$$\frac{\delta q_x}{\delta x} + \frac{\delta q_y}{\delta y} + \frac{\delta q_z}{\delta z} - W^* = -S_s \frac{\delta h}{\delta t} \qquad \text{Equation 2-3}$$

Where:

q_x, q_y, q_z are Flow rate in x,y,z direction.

W is the volumetric inflow rate per unit volume.

S_s is the specific storage or the rate of water replenished or depleted for every unit change in aquifer head volume.

t is the time.

Right-hand side term $\left(S_s \frac{\delta h}{\delta t}\right)$ is taken as zero for the study state condition and flow rate in equation 2-3 can be rewritten as:

$$q_x = -K_x \frac{\delta h}{\delta x}$$

$$q_y = -K_y \frac{\delta h}{\delta y}$$

$$q_z = -K_z \frac{\delta h}{\delta z}$$

Where:

K_x, K_y, K_z are components of hydraulic conductivity in x,y,z direction.

Numerical groundwater flow modeling uses these partial differential equations that describe three-dimensional groundwater flow in an aquifer. These techniques involve dividing the subsurface into a grid of cells and solving mathematical equations to simulate the flow of water between these cells. The models take into account factors such as hydraulic conductivity, topography, and boundary conditions to accurately predict groundwater movement.

Complex groundwater flow systems that cannot be analyzed only through analytical solutions can be better understood with numerical groundwater models. They offer an efficient method for investigating important properties of groundwater dynamics, including:

- Direction and velocity of flow particles of groundwater.
- Formulation of depression cone and extraction of water on drawdown.
- Infiltration of seawater into the groundwater system.
- Particle tracking of contaminated water from its originated sources.
- Effect of different climate seasons on the aquifer recharge.
- Testing of artificial recharging methods.

By calibrating using site-specific data, numerical models are capable of accurately predicting how groundwater sources would react to new conditions, such as increased pumping rate.

2.6 Boundary and Initial Conditions

The boundaries of a numerical groundwater model simulate groundwater flow and establish its limitations. They represent the hydrological interaction between the model area and the surrounding environment. These conditions can include the inflow and outflow of water, the presence of barriers or boundaries that restrict water movement, and variations in groundwater levels due to natural or man-made factors. They help capture the complex dynamics of water movement and ensure that the model results align with real-world observations. Boundary conditions can be divided into three categories:

2.6.1 Specified Head Boundary

Specified head boundary is a type of boundary condition where a fixed head value is assigned to nodes along the model boundary based on known field conditions. During the simulation, the head value remains constant at the specified level. Physically, it represents boundaries that are connected to a recharge or discharge source, so the head does not fluctuate. Common scenarios include model boundaries connecting to river and lake.

2.6.2 Specified Flow Boundary

In the modeling process, this boundary condition assigns a fixed flow rate across nodes along the model boundary rather than a set head value. This condition is used in a situation where the flow rate remains constant while allowing the head to float during the simulation. When there is no flow between boundary nodes and surroundings, this is referred to as a no-flow boundary condition. Commonly specified scenarios include one-way flow, such as seepage and underground aquifer flow. Flow is calculated from Equation 2-4.

$$\frac{\delta h}{\delta \gamma} = -\frac{q_\gamma}{K_\gamma} \qquad \text{Equation 2-4}$$

2.6.3 Head Dependent Boundary

It is also known as a mixed boundary condition because the head or flow varies depending on field conditions and conceptual understanding. These conditions can include rivers or streams that have varying water levels due to rainfall or seasonal changes. This condition allows the model to accurately simulate the effect of changes in water levels on groundwater flow for different stress periods. The flow equation is derived from Darcy's equation, where the gradient is calculated as the difference between the hydraulic head on the end node and the specified head outside the boundary. Finalized form is shown in Equation 2-5.

$$q_\gamma = -K_\gamma \frac{h_b - h_{i,j,k}}{\frac{\Delta_\gamma}{2}} \qquad \text{Equation 2-5}$$

2.7 Model Calibration

In numerical groundwater modeling, calibration is a key phase in which model parameters are gradually changed within acceptable boundaries until the model simulation outcomes closely resemble actual data collected from the field. The accuracy and reliability of the groundwater model depend on it. It involves adjusting major input parameters like hydraulic conductivity and recharge rates to achieve a better fit between the model predictions and observed data (Anderson et al., 2015). It is an iterative process that requires careful analysis and comparison of the model results with the field measurements and may involve multiple iterations to achieve satisfactory results. The initial simulation gives an approximate visual of the starting point for calibrating a model's hydrogeological properties and boundary conditions. The errors identified in groundwater levels, flow and other outputs during the calibration process are used to refine the model by adjusting the parameters (Anderson et al., 2015). The next iterations involve refining the input parameters based on the comparison of model predictions with observed data, resulting in a more accurate simulation of field conditions.

Numerical model calibration can be done in a number of ways. Traditionally, manual calibration has been used because it allows hydrogeologists to apply their in-depth understanding of a site condition during the calibration process, allowing more interactive and knowledge-driven adjustments of parameters. However, manual calibration can be time-consuming and subjective, as it relies heavily on the expertise and judgment of hydrogeologists (Boyle et al., 2000).

Alternatively, automated calibration methods like PEST (Parameter Estimation) have been developed to streamline the process and reduce human bias by using optimization algorithms to iteratively adjust model parameters until a satisfactory match between predicted and observed data is achieved. This method has proven to be efficient and timesaving, especially when dealing with complex hydrogeological models (Doherty, 2003). Additionally, the use of automated calibration methods can also help in handling large datasets and reducing

computational costs. In general, factors like the study's objectives, computational needs, and model complexity affect the choice of calibration technique.

3

Case Study Site

An overview of the case study area is provided in this chapter, covering the site's location, topography, geology, hydrogeology, and catchment area. This information mainly draws from the Geological Survey of Sweden (SGU), web site.

3.1 Conceptual Site Model

The Kankberg Mine is located at latitude 64º55’20” N longitude 20º16’3.7” E, is a foothill area in northern Sweden, near the town of Boliden. This polymetallic mine is operated by Boliden Mineral AB. The estimated total reserve of this mine is 10.30 million tons which includes tellurium (Te), gold (Au), silver (Ag), and other important minerals. The site covers an area of approximately 4 square kilometres and encompasses both underground and open-pit mining operations as shown in Figure 3-1.

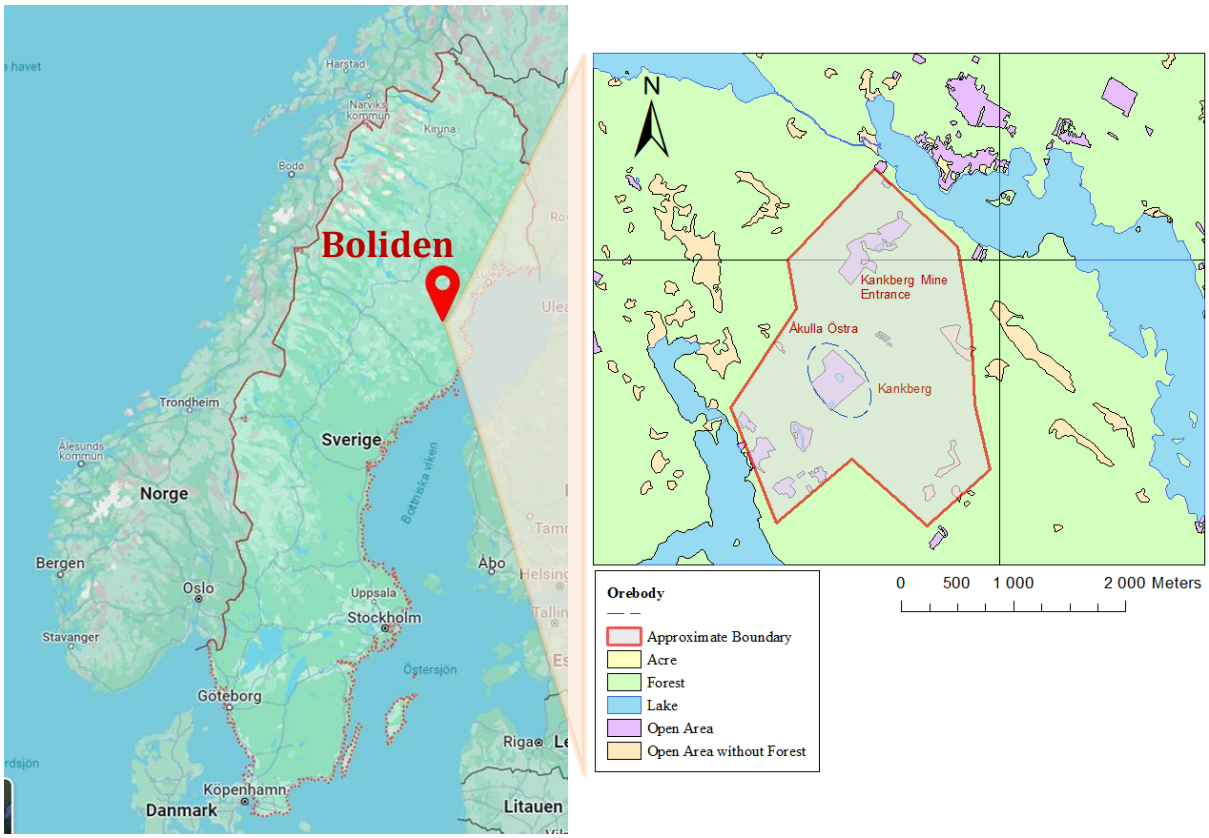

Figure 3-1. Map of Kankberg mine. (SGU, 2023).

At Kankberg, the first explorations of the deposit were conducted in 1927 at the Åkulla Östra site (Voigt & Bradley, 2020). Over the years, the mine has undergone several expansions and modernization, which has allowed it to increase production and improve efficiency. In 2009,

they started a new drilling campaign beneath Åkulla Östra and production started in 2012, known as Kankberg underground orebody, as shown in Figure 1 (Voigt & Bradley, 2020). They are currently carrying out mining operations between -300 and -600 meters below the surface. They intend to obtain authorization to mine down to the -1,000 meters level (Voigt & Bradley, 2020). This mine is an important source of metal production in Sweden, providing jobs and economic benefits to the local community. The mine's production of Te, Au and Ag has been important for the Swedish economy and has been one of Boliden's major revenue sources.

3.2 Topography

The topography and license exploration area of the Kankberg mine are presented on the Mineralrättigheter map in Figure 3-2. The coordinate grid according to the Swedish standard used for the map is SWEREF 99 TM (SGU, 2023). The surrounding landscape is characterized by rugged terrain with steep slopes, rolling hills, and numerous valleys and lakes. Kankberg Mine is densely forested, with a mix of coniferous and deciduous trees that provide a habitat for a variety of wildlife species. According to Swedish Geological Survey (SGU) the elevation ranges from over 200 m to 285 m above sea level for this region. The closest residential area, Kankberg Town, is located on the other side of the lake Bastuträsket, approximately 1000 m from the mine.

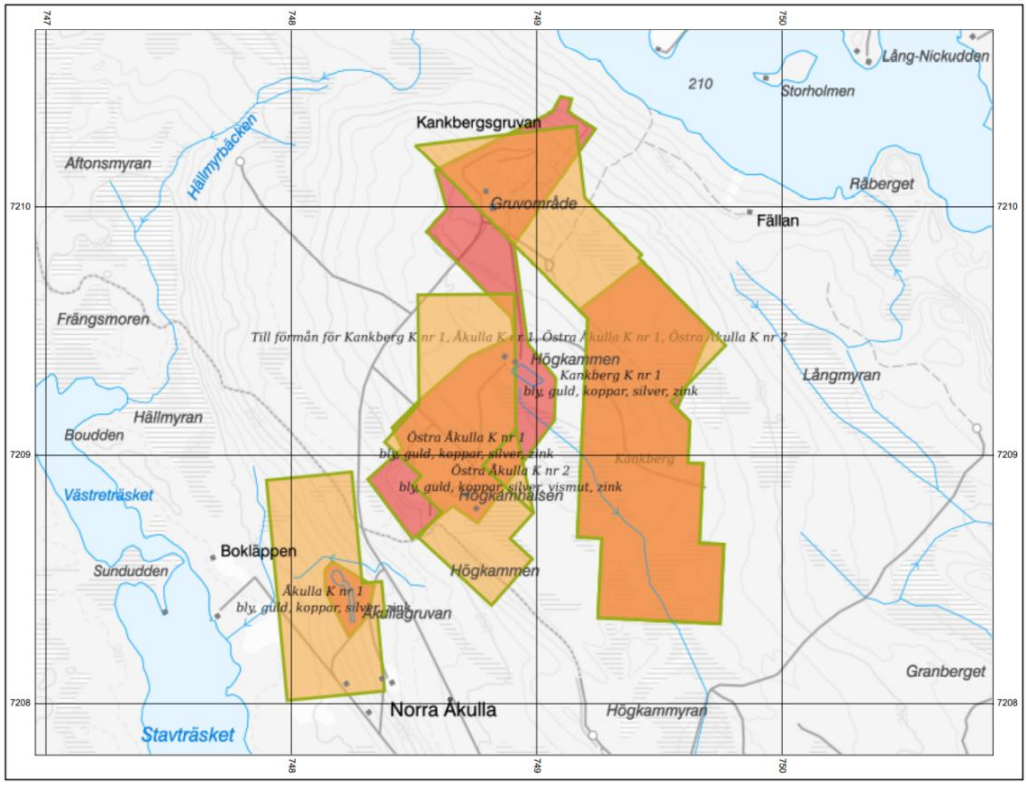

Figure 3-2. Map showing the Concession permit area for the operational Kankberg mine and adjacent concession permits. (SGU, 2023).

3.3 Hydrology & Hydrogeology

The hydrological conceptual model for the Kankberg mine is shown in Figure 3-3. In this conceptual model, precipitation is the only source of water in this area. This precipitation falls as rain or falls as snow, which can either runoff onto the catchment area or infiltrate into the subsurface rock. There are four sub-catchment areas in this region. Since the dividing ridge goes through the center, there are mainly two specific directions of flow, NE and SW in this region as shown in Figure 3-4. The primary hydrological factors that influence the water balance of Kankberg Mine are surface runoff and infiltration. Two nearby water bodies, Bastuträsket in the northeast and Stavträsket in the southwest, serve as recharge boundaries for the area.

Kankberg Village, is located on the other side of the lake Bastuträsket, approximately 1000 m from the mine. The Boliden company owns all the houses in the village, but they are unoccupied.

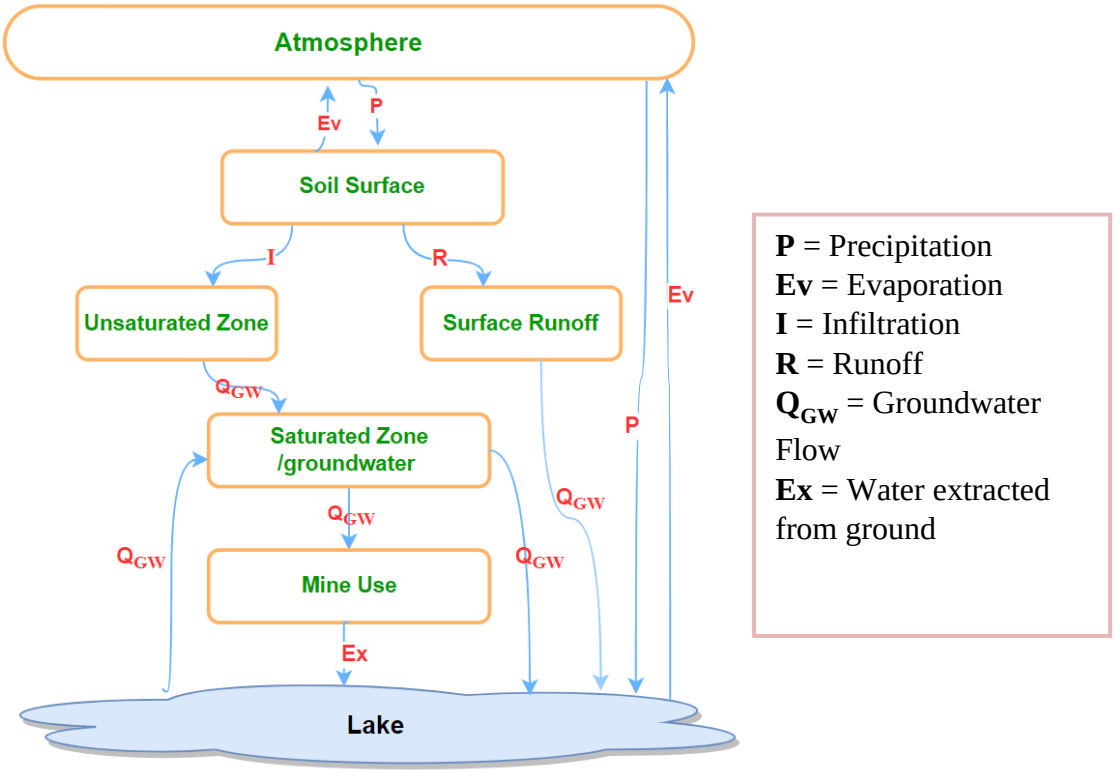

Figure 3-3. Conceptual model of the hydrology of Kankberg area.

The annual average temperature in this area is 1.9°C, and it drops to lowest average of -12°C in January or February and reaches its highest average level of 21°C in July (Voigt & Bradley, 2020). Winter conditions can be challenging in this area with daylight lasting only 4 hours while in summer, days can last up to 21 hours.

According to the last 30 years of SMHI data, the average annual precipitation of sub-catchments in this area is around 715 mm, the average annual evaporation is around 417 mm, and the average annual runoff is around 298 mm. As per Swedish Geological Survey data, bedrock have a hydraulic conductivity of 4.57×10^{-7} m/s, and as per SGU well register the average well capacity in this area is less than 15 m^3/day. Because the surface of the area consists of moraine unconsolidated deposits, it has a medium level of permeability. This type of soil is formed by the deposition of rocks and sediments carried by glaciers. The varying-sized particles in moraine deposits create pore spaces that allow for water movement and aeration. It allows water to slowly seep through, providing a suitable environment for vegetation growth. Additionally, the medium level of permeability helps in preventing waterlogging and facilitates drainage in the area. This type of deposits is often found in areas that were once covered by glaciers, such as valleys and plains and is highly fertile due to the deposition of minerals carried by the ice.

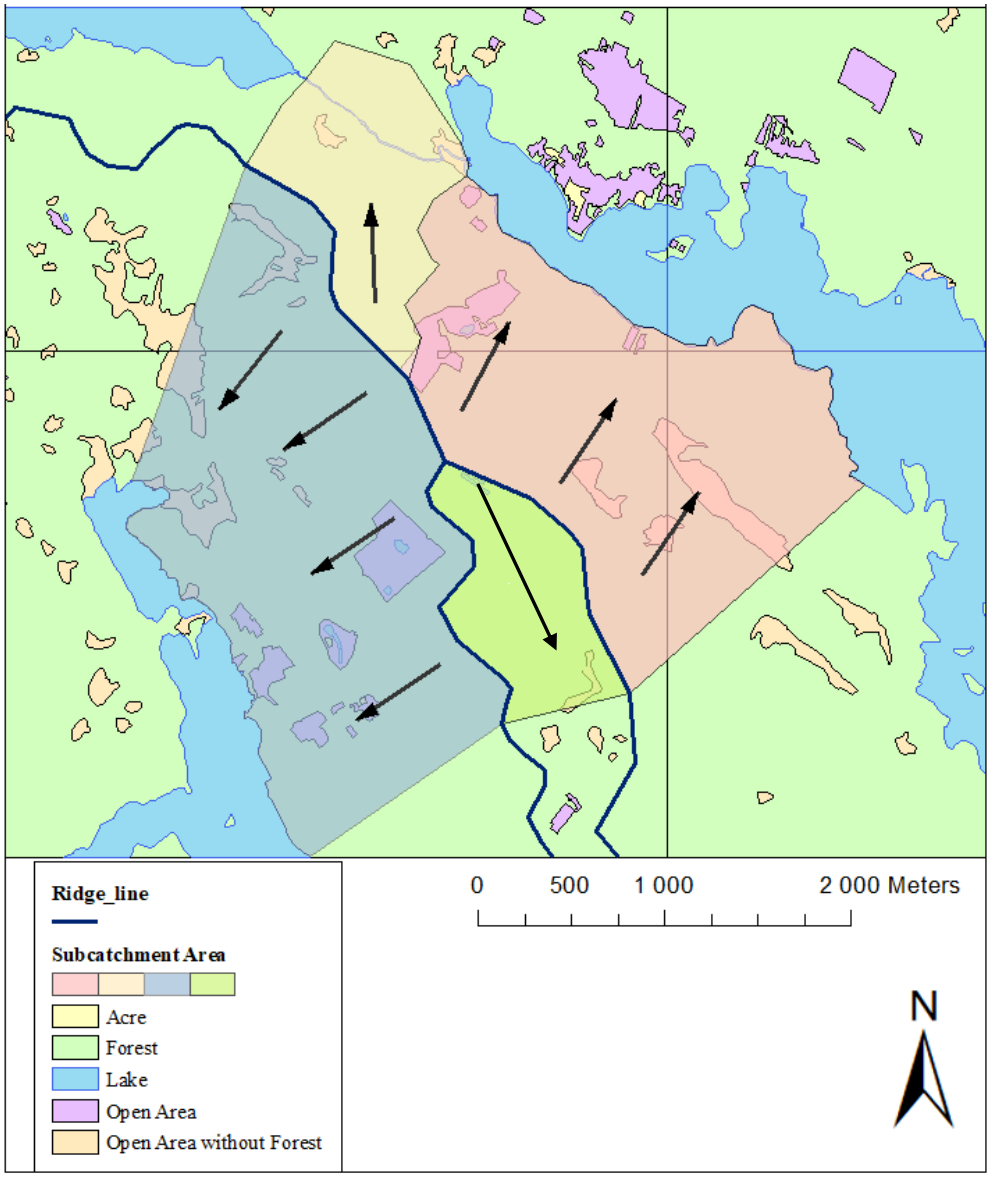

Figure 3-4. Sub-catchment area at Kankberg mine. (© Lantmäteriet).

3.4 Geology

The mine is located in the northwest corner of Skellefteå district, which is known for its rich and diverse minerals. The geology of the Kankberg Mine area is characterized by a complex mixture of low to medium metamorphic rock in the Baltic Shield (Allen et al., 1996). Figure 3-5 shows the geological structures in the area include fold, deformation lines and structural lines. The rocks are brittle in nature and has vertically tendency.

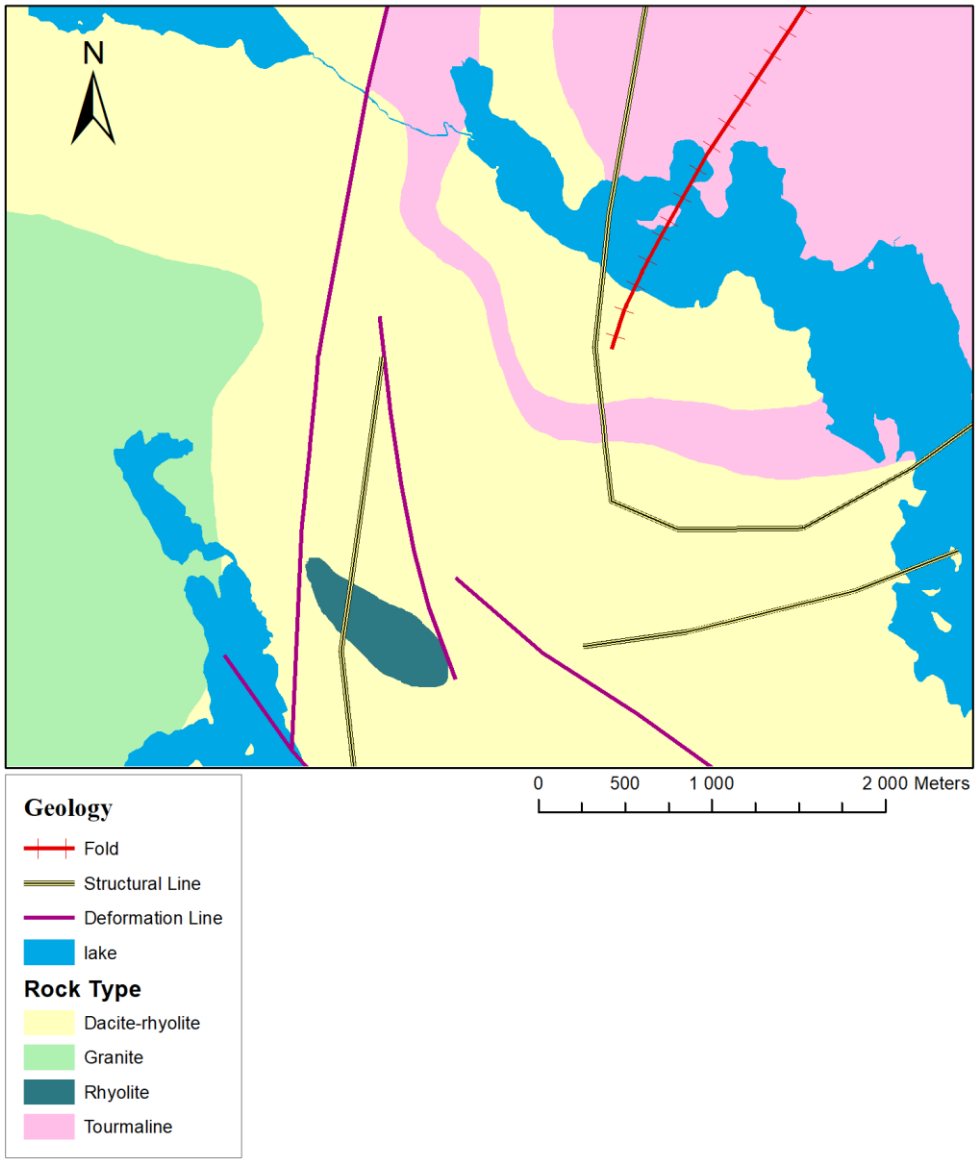

Figure 3-5. Geological Structure on this region. (© Lantmäteriet).

The mineralization primarily occurred 1.87–1.92 billion years ago due to subaqueous rhyolite cryptodome-tuff volcanoes (Allen et al., 1996). These subvolcanic dykes have resulted in the formation of ore deposits in the area. The size of these rhyolite volcanoes varies from 2 to 10 km in diameter. The mineralization is characterized by high-grade zinc, lead, and silver, with minor amounts of copper and gold (SGU, 2023).

The majority of the unconsolidated deposits on the surface consist of glacial till but there are some patches of peat in this area. The average depth of unconsolidated deposits varies from 3 to 5 meters (SGU, 2023). The presence of high-grade mineralization, combined with the geological structures in the area, makes Kankberg an attractive target for mineral exploration and development.

3.5 Contaminants of Concern

The Kankberg Mine's geography presents a number of challenges to mining operations, including the need to manage water supply. The company, Boliden Mineral AB, ensures the safety and security of contaminants spread in the area by enforcing the local authority's policies or regulations about acceptable risk level. Because the materials being extracted are only rocks, and cutting and filling techniques are being used, the possibility of subsidence was not even an issue for the site. The drainage water used during the operation is the most common and significant contamination in this ecosystem. To mitigate this, a treatment plant has been constructed at Kankberg site as shown in Figure 3-6, to purify the drainage water before releasing it back into the environment. This treatment plant reduces the amount of acidic water due to sulphates and heavy metals like copper, lead and zinc in the drainage water to an acceptable level. Additionally, the hydraulic gradient into the mine serves as a safety measure that prevents leachates to the environment.

Figure 3-6. Water treatment plant at Kankberg site.

However, after the service life of the mine contamination will become an issue when the groundwater level is restored to its original level and the natural gradient enables groundwater to flow out of the area. after the service life of the mine. In terms of air quality, energy consumption is a major contributor to carbon emissions. Although Kankberg mine consumes way less energy than other mines, they are still trying to make a difference in this industry. Recently, they installed a heat exchanger that used heat from the exhaust vent to warm up the inlet air. This technique will reduce 85% of LPG consumption and restrict CO2 emissions to 60% by 2030 (Boliden, 2022).

4

Methodology

In this chapter, the strategy applied for modeling the study area is presented, along with an overview of the essential data required for the simulation.

4.1 General Strategy

The research method employed for this study involves a comprehensive approach focusing on the modeling of underground water flow while accounting for the influence of surrounding surface water bodies and precipitation infiltration. This methodology integrates two distinct data sources: publicly available open data and data acquired through field investigations. The primary emphasis is on groundwater modeling using open-source data. Subsequently, a second model is crafted utilizing field data. Finally, a comparative analysis of the two models is conducted to find the accuracy that can be attained using open-accessed data.

To conduct the simulation, MODFLOW-2005 which is a finite-difference groundwater flow modeling program developed by the United States Geological Survey (USGS) has been selected. MODFLOW solves the groundwater flow equation for porous media and assumes subsurface flow occurs through interconnected pore spaces and fractures that effectively behave as a porous medium. For this study, the fractured rock at Kankberg has been assumed to be a porous medium. Furthermore, Newton-Raphson formulation for Water-Table Flow (NWT) has been selected as the solver. This choice enables the utilization of advanced numerical techniques, making it possible to simulate and analyze the intricate dynamics of underground water flow, considering the complex interplay between precipitation, geological factors, and mine-related activities. The working process which was used in this project is presented in Figure 4-1.

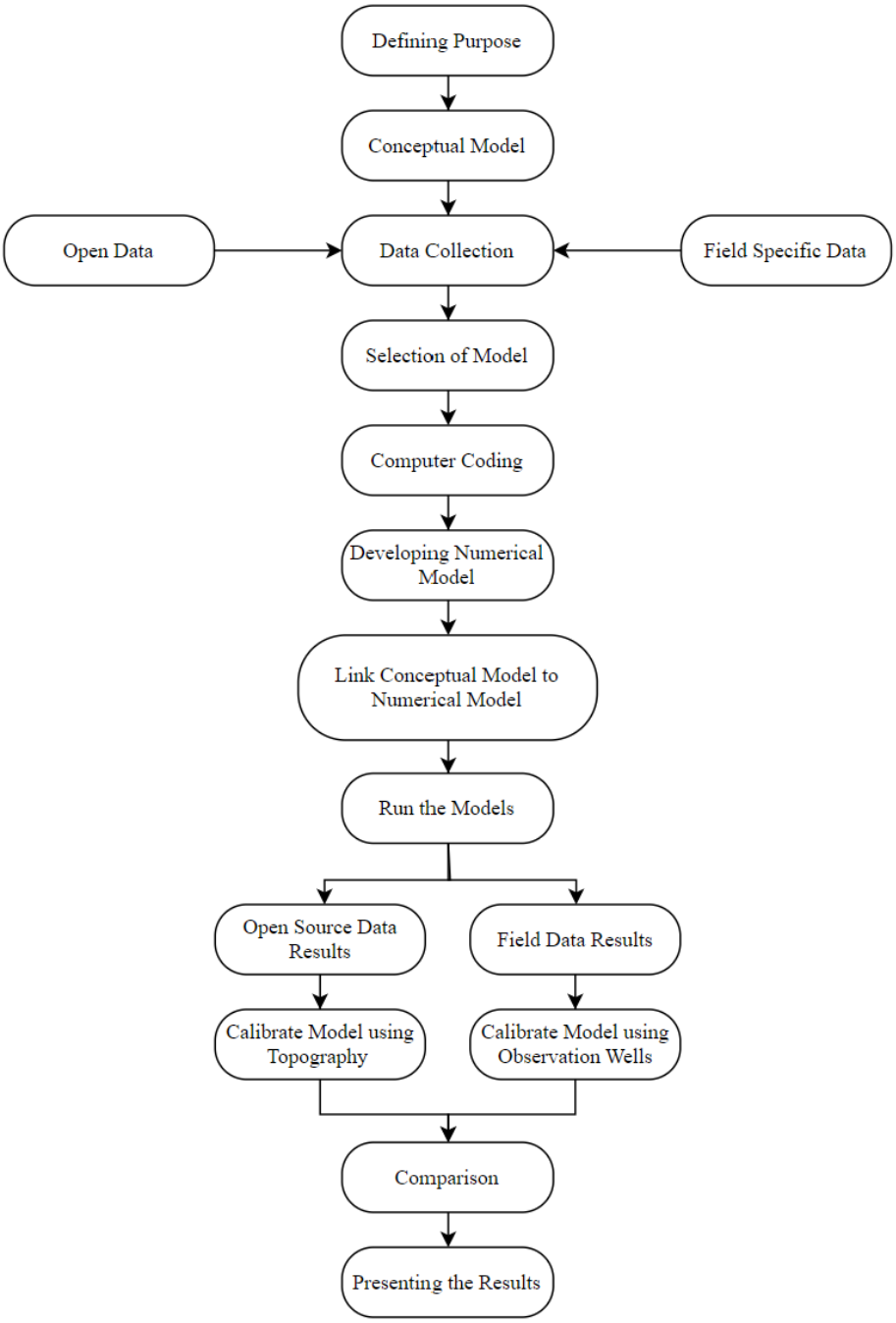

Figure 4-1. Workflow for groundwater modeling inspired by (Anderson et al., 2015).

4.2 Data collection

Geological, hydrogeological, and hydrological data related to the Kankberg site were primarily extracted from open-access information. The topographical data and hydraulic conductivity value for the rock close to the ground surface were obtained from the Sveriges lantbruksuniversitet (SLU) website (Lantmäteriet, 2019). However, for rocks at greater depth and distant from the ground surface, there is a lack of data. Recognizing the gradual decrease in hydraulic conductivity with greater depth - since increased depth is associated with higher

rock pressure, leading to a reduction in the width of water-bearing fractures and consequently fewer fractures - assumptions have been made to address this data gap. Precipitation data was obtained from the SMHI website (SMHI, 2022) with a 60% reduction to account for the omission of covering soil in the modeling process (Appels et al., 2015), focusing solely on the underlying rock. Information concerning the mine's depth, presumed to align with the aquifer base, was derived from a graph provided by Boliden (Wladis, 2008) which can be seen in Appendix A.1. Furthermore, the field investigation data is obtained through the reports of Kankberg (Wladis, 2008). The data for both models can be seen in Table 4-1 and later in Table 4-2. The location of observation wells used for site-specific data model are show in Figure 4-2.

Table 4-1. Hydraulic head of observation wells used in site-specific data model.

Well ID	Head (m)	Depth (m)	Latitude	Longitude
Well 1	215.23	225	7209590	748470
KA2103B	219.9	199	7209148	749058.3
KA2104B	234.75	199	7208764	748789.1
KA2106B	188.73	199	7209056	748443

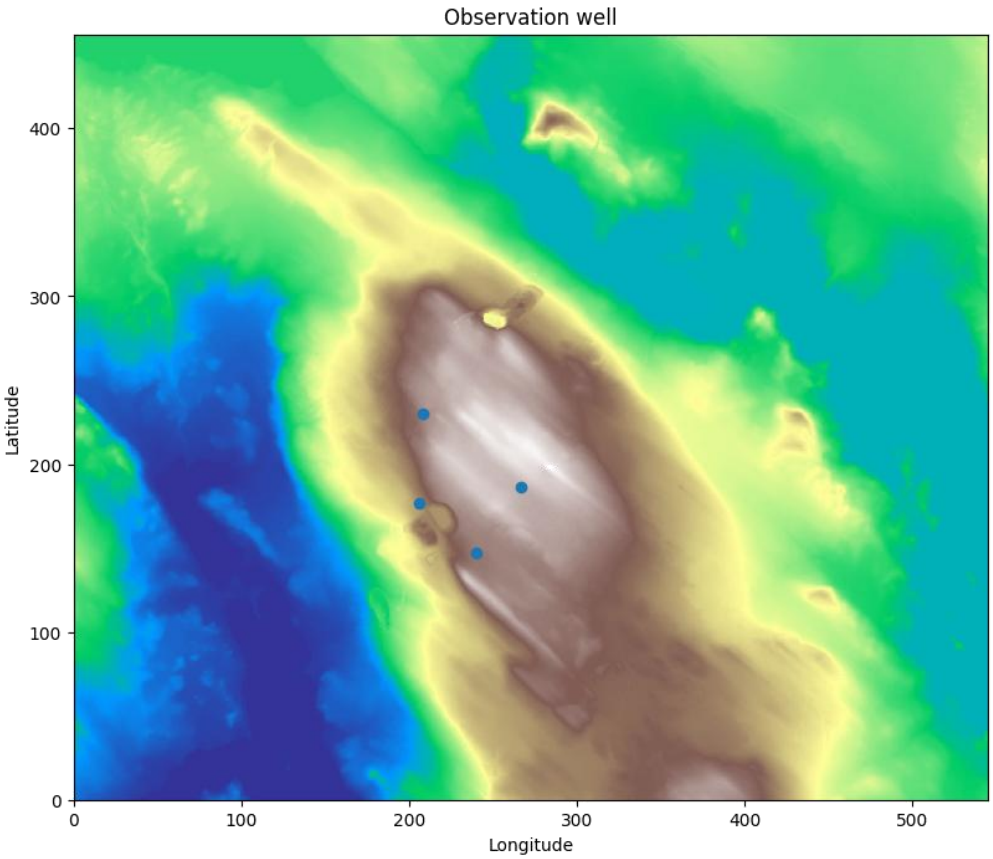

Figure 4-2. Location of observation wells used for site-specific data model. (© Lantmäteriet)

4.3 Numerical model development

To simulate the groundwater flow using MODFLOW-2005 with NWT solver, the following essential steps must be undertaken and the script for both models can be found in Appendix B.

4.3.1 Defining the discretization

To initiate the simulation, the first crucial step is the definition of discretization parameters. In this context, a grid network with 5 layers (z-axis), 456 rows (y-axis), and 545 columns (x-axis) is chosen for the representation of the model. It should be noted that the dimensions in the x and y directions are calculated by assigning a grid size with a spatial resolution of 10 x 10 m^2 to the bedrock elevation map of the study site.

4.3.2 Assigning the geology

To accurately represent the geological characteristics of the study area within the model, it is important to consider the stratigraphy of both the unconsolidated deposits and bedrock layers. Nevertheless, in simplifying the model and acknowledging the relatively thin deposits thickness, approximately 5 m, which does not extend across the entire rock surface, the unconsolidated deposits layer is excluded from the model consideration.
Geological investigations have revealed significant variations in rock fracturing at different depths. As a result, the geological composition of the site can be effectively characterized by five distinct layers in the rock, as shown by the cross-sectional model in Figure 4-3. Each of these layers exhibits distinct characteristics and hydraulic conductivities (see Table 4-2).

1. Layer 1 - weathered material: layer 1 predominantly consists of friable, weathered material. This layer is characterized by lower structural integrity and higher porosity, making it more susceptible to the flow of groundwater. This results in increased hydraulic conductivity and a well-connected network of fractures. It is assumed that this layer covers a depth equivalent to 90% of the bedrock DEM (digital elevation model).

2. Layer 2 - transitional zone: layer 2 represents the transitional zone between weathered material and solid bedrock. It shows intermediate hydraulic conductivity compared to layer 1 and the deeper layers. The depth of 0.7 times bedrock DEM marks the boundary where geological conditions shift towards less fractured bedrock.

3. Layer 3 - fully solid bedrock: layer 3 comprises fully solid bedrock with significantly reduced hydraulic conductivity compared to the overlying layers. With a thickness that is equal to 45% of the surface bedrock elevation, this layer represents the zone where the rock is relatively unaltered and solid.

4. Layer 4 – bottom layer of mine: layer 4 represents the bottom of the mine and it is only considered to make the model more flexible for assigning the properties and calibration. The bottom of the mine is located 600 m below the ground surface.

5. Layer 5 - aquifer bottom: layer 5 marks the base of the aquifer, featuring solid bedrock with a low hydraulic conductivity. This layer is incorporated into the model to ensure that groundwater flow is unaffected by the model's depth. The depth of layer 5 is determined by the variable AcuifInf_Bottom, which is defined at -1000 and aligns with the aquifer's lowermost elevation.

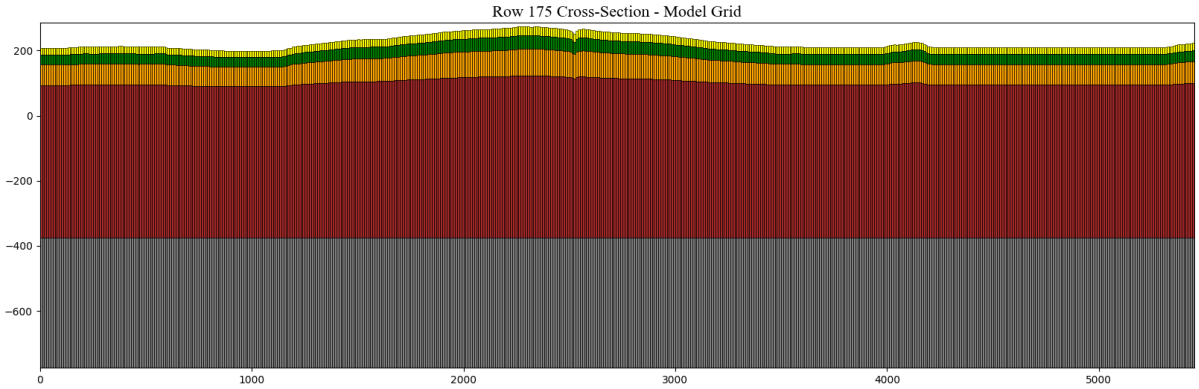

Figure 4-3. Cross-section of the model with the grid and bedrock layers visible.

Table 4-2. Collected data for simulation.

Open-Source Data				**Field Data**		
Depth	Thickness (m)	Hydraulic Conductivity (m/s)	Recharge (mm/yr)	Thickness (m)	Hydraulic Conductivity (m/s)	Recharge (mm/yr)
0-22	22	3.47e-6	150	22	1.80e-06	150
22-56	34	4.57e-7	-	34	2.53e-07	-
56-124	68	2.47e-8	-	68	9.25e-08	-
124-600	476	1.11e-9	-	476	6.93e-08	-
600-1000	400	2.11e-10	-	400	3.00e-10	-

4.3.3 Assigning the hydraulic properties and recharge

In this step, hydraulic conductivities (K) for the different layers are assigned to the model based on rock type, assuming an isotropic aquifer. The hydraulic conductivity values used for site-specific data for different layers were taken from the Wladis (2008), and details of boreholes are presented in Appendix A.2. For the 2nd layer, the k value is calculated using

information obtained from SGU (SGU, 2023), which is log(K) = -6.34. Subsequently, this value is used as a reference point for determining the hydraulic conductivities of the remaining layers. The uppermost layer, being closer to the surface, experiences more weathering and contains a higher density of fractures, resulting in higher K values. In contrast, the layers beneath are more compacted and solid, containing fewer fractures, leading to lower hydraulic conductivity. It should be noted that the model operates under the assumption of steady-state flow, and as a result, specific storage and specific yield do not play a role in influencing the model outcomes and are consequently excluded from consideration.

As mentioned earlier, the average recharge value for the case study is around 298 mm/year. However, since the model excludes the deposits covering the rock, it is necessary to account for a reduced recharge rate. (Appels et al., 2015) suggest that 60% of the total recharge should be attributed to the top layer of bedrock. (Chand et al., 2004) conducted a study indicating that weathered granites, under average rainfall of 968mm, show a recharge rate ranging from 6-200 mm/year. Based on these studies, an initial estimate of 103 mm/year for the recharge value is proposed.

4.3.4 Boundary condition

Boundary conditions in the model are determined by the geological and hydrological characteristics of the case study, as illustrated in Figure 4-4. The maps of the region reveal the presence of three lakes: namely, Bastuträsket, Stavträsket, and Klockträsket, with constant head levels of 210, 191, 217 meters, respectively.

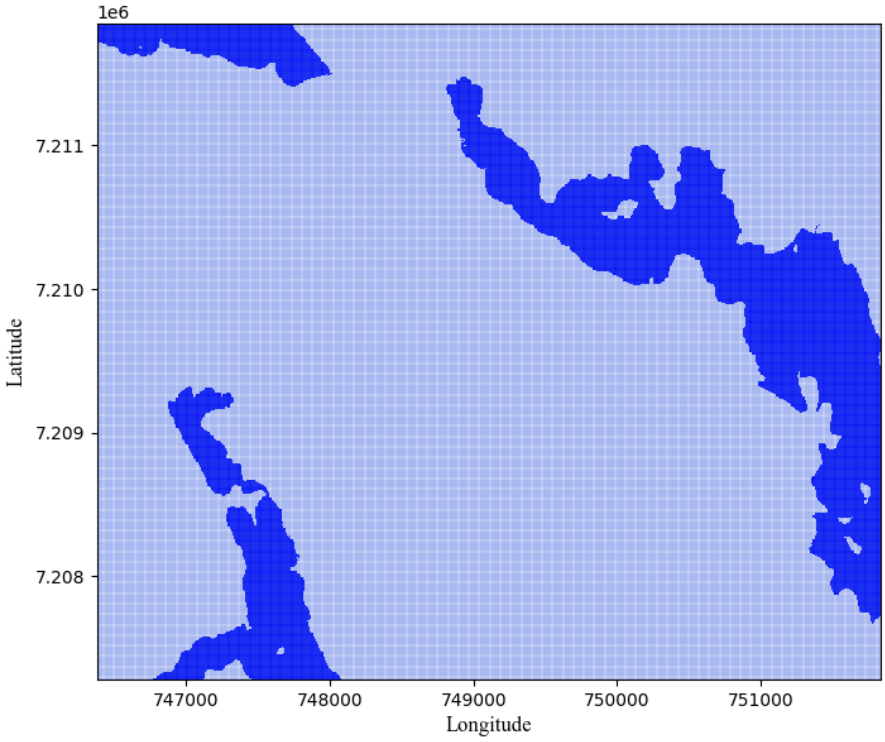

Figure 4-4. Location of different boundary conditions in the MODFLOW.

4.3.4.1 Drainage

The mine was roughly modeled in an elliptical volume from which groundwater was simulated to be extracted. This simplified geometry provides a representation of the outline of the actual mine shown in Appendix A.3. This drainage pattern was described by the standard form equation of an ellipse:

$$\frac{(x-h)^2}{a^2} + \frac{(y-k)^2}{b^2} = 1 \qquad \text{Equation 4-1}$$

In this equation, the ellipse is centered at the coordinates (h, k), and it is defined by its semi-major axis (a) and semi-minor axis (b), both aligned with the Cartesian plane. As an initial attempt, values of a and b that cover 30 and 20 grid cells, respectively, are chosen. It is important to note that the dewatering of the mine was implemented starting from the third layer of the model and no drainage was considered for the first two layers. The location of the drainage is illustrated in Figure 4-5.

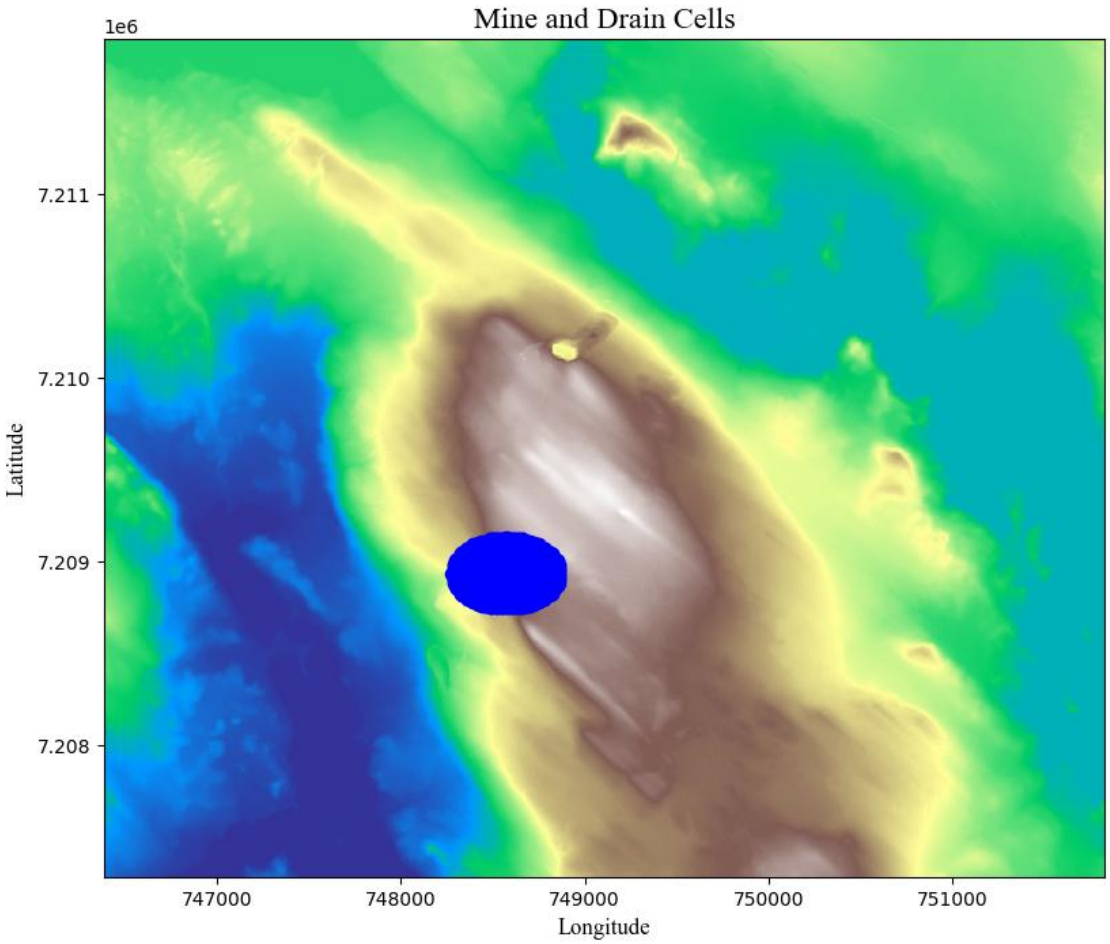

Figure 4-5. Blue ellipse represent the location and shape of the drainage.

4.4 Calibration

After the initial run of the first model using the open-sourced data, a manual calibration process was done to ensure that the water head in various locations reflected the topography of the site. This is to enhance the model's performance and bring it into closer alignment with real-world conditions. For the majority of the area, 70 mm per year of rock recharge satisfies this criterion, but there are some patches where water overflows the surface, as shown in Figure 4-6. To control this problem, different recharge values are used to control overflow. Around the mine, a higher recharge value is used because water will be extracted due to the mining operation, and this area will absorb more water than the rest of the area.

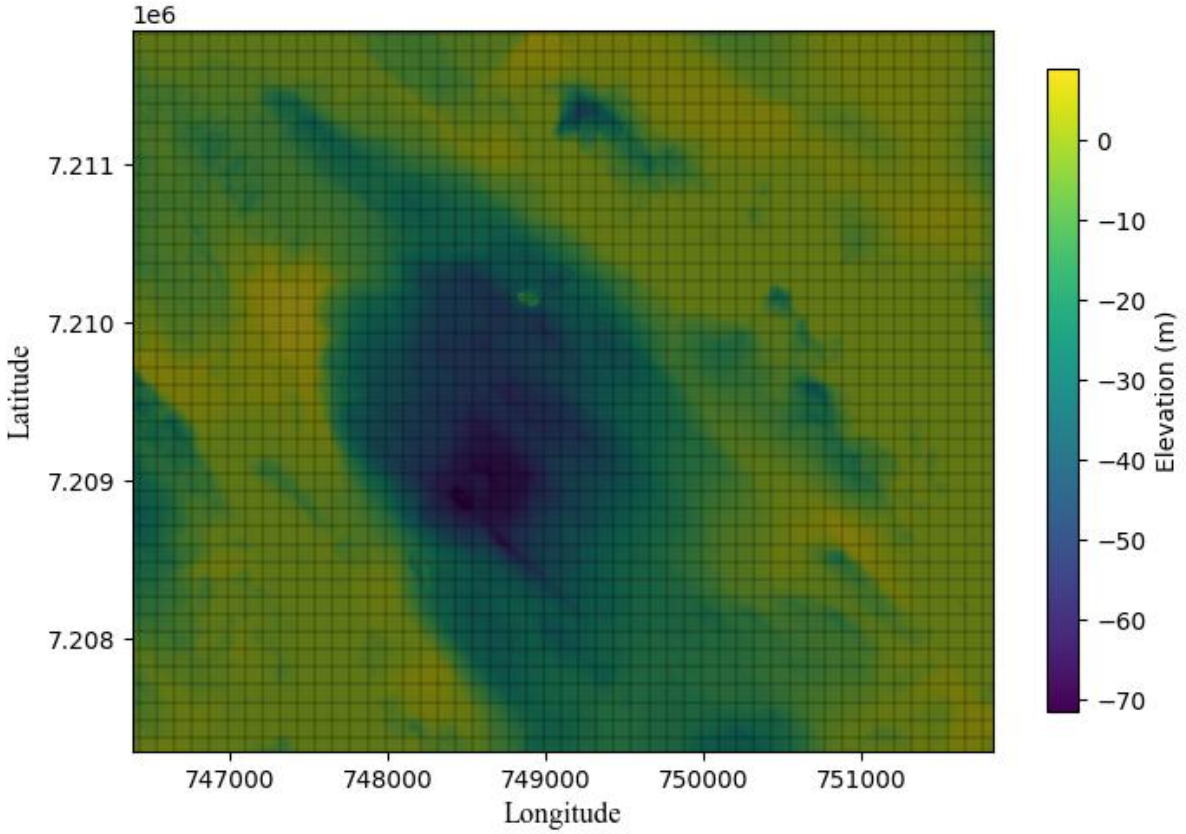

Figure 4-6. Water level (m) without differential recharge.

For the second model, constructed using field-investigated data, emphasis was placed not only on adjusting hydraulic parameters but also on accounting for real-world drainage conditions. The study area experiences an overall constant drainage rate of 80 m^3/h, of which mine contributes around 25 m^3/h and the rest comes from 3 vertical shafts and the ramp area. Consequently, it is crucial for the calibrated parameters to effectively accommodate this drainage within the system. Additionally, the calibration process incorporated head values from four observation wells, as detailed in Table 4-1, with the aim of minimizing the disparity between simulated and observed heads.

Figure 4-7 shows the final calibration phase that involved careful and repeated adjustments of key hydrogeological parameters, with a special focus on hydraulic conductivity and recharge. The object of calibration is to identify the optimal combination of parameter values that reflect the topography of the area and simultaneously allow water to flow in a manner that represents a reasonable drainage value for the mine.

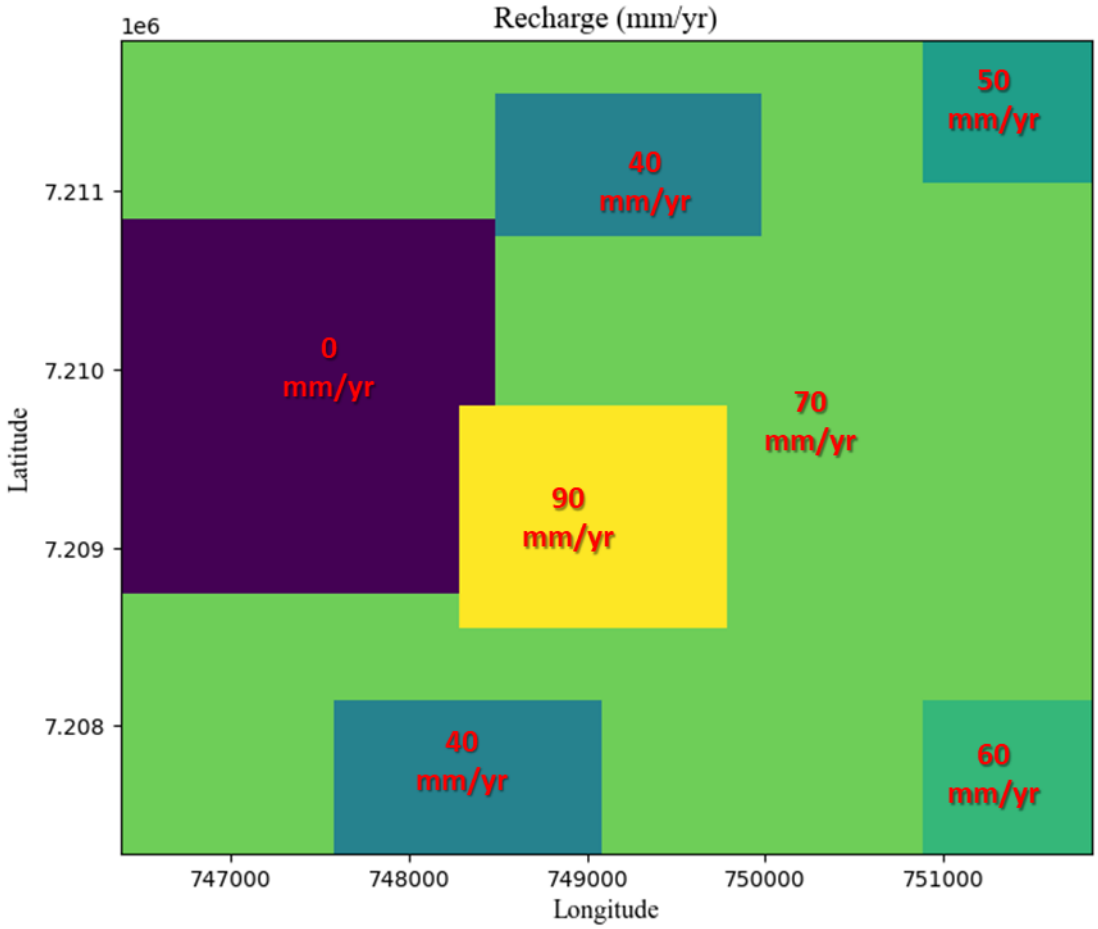

Figure 4-7. Recharge for the first model after calibration.

5

Results

This chapter provides an analysis of model outputs to evaluate the accuracy of a numerical groundwater model using open-source data in comparison to using field-calibrated data for the Kankberg mining project. The aim of this section is to compare the reliability of a model based on open-source data to a model based on site-specific data, and to evaluate the potential impacts of mining activities in terms of drawdown and flow direction, as well as to gain a better understanding of the subsurface condition of this site. The hydrogeological field studies involved collecting data of groundwater levels at various locations and flow rates at different levels within the project area. This data was then used to develop a numerical groundwater model that simulates the movement of groundwater and predicts its behaviours. The comparison between models using open-source data and site-specific data, respectively, provides valuable insights into the reliability of existing information and helps in identifying any gaps or uncertainties that need to be addressed.

Four observation wells are used to collect data for the site-specific model, and data for the open-source model is collected from the SGU and SMHI websites. The geology and topography of a two-dimensional site were constructed using open-source data from SLU website. The open-source data model was calibrated roughly based on water levels looking reasonable compared to land topography, and then a more detailed calibration for the site-specific data model was done using water level observations. After that, the calibrated model was used to simulate both situations for a steady state situation. The model predictions provide a valuable understanding of drawdown due to the mine and water flow locally for different stratigraphic layers.

Table 5-1 presents a comparison of groundwater head predictions from the open-source data model and site-specific field data model. This table lists the measured field head values at each of the 4 observation wells, along with the simulated heads from the open-source data model and the field-specific data model. An additional column shows the percentage accuracy of each model's simulation compared to actual field measurements. In the end, the root mean square error (RMSE) is presented, which allows us to assess the overall performance of our models and helps us make conscious decisions based on their accuracy.

Table 5-1. Groundwater head predictions and their % accuracy.

Well ID	Actual head (m)	Simulated head of open-source data (m)	% accuracy of open-source data	Simulated head of site-specific data (m)	% accuracy of site-specific data
Well 1	215.23	219.3	98.1	210.7	97.9
KA2103B	219.9	227.6	96.6	220.9	99.5
KA2104B	234.75	221.5	94.4	217.8	92.8

KA2106B	188.73	222.4	84.9	216.1	87.3

The root mean square error (RMSE) is a commonly used statistical method for calculating the average modeling calibration error. RMSE is calculated by taking the square root of the average of the squared differences between observed and simulated values. The RMSE provides a single value that represents the average error between observed and simulated groundwater head values. A lower RMSE indicates a better fit between the model predictions and field data. The RMSE for every model is determined using Equation 5-1, and the results are displayed for each model in Table 5-2.

$$RMSE = \sqrt{\frac{1}{n}\sum_{i=1}^{n}\left(Y_i - \widehat{Y_i}\right)^2} \qquad \text{Equation 5-1}$$

Where:

- Y_i is the actual measured groundwater head value.
- $\widehat{Y_i}$ is the corresponding head value simulated by the model.
- n is the total number of observation points used for calibration.

Table 5-2. Root mean square error for each model.

RMSE	**Open-source data model**	**Site-specific data model**
	18.6	16.2

The root mean square error (RMSE) has been calculated using four observation wells, RMSE between the simulated and observed groundwater heads was computed in order to assess the calibration accuracy of both models quantitatively. The RMSE value of 18.6 was obtained using the open-source data model, suggesting a greater average error between the simulated and measured heads throughout the wells. In contrast, once the model was created utilizing site-specific field data, the RMSE was 16.2. The results indicate that the overall site-specific data model provided a more accurate simulation than the open-source data model. This suggests that the site-specific data model is more effective in capturing the unique characteristics of the field. However, the open-source data model is not that far from the site-specific data model and can still provide sensible predictions.

It is important to consider the impact of outliers like KA2106B on the overall accuracy of the models. Because of a single well, the accuracy of both models is reduced, and the RMSE indicates a higher value. The results from both models are significantly improved once this well is removed from the RMSE calculation. After excluding this outlier, both models show a factor of difference, the new RMSE value is around 8. This outlier's large difference can be explained by the fact that this well can be situated close to a relatively large rack, which lowers its water level.

The inflow into the mine will determine how the mine dewatering will affect the groundwater and surrounding environment. Appendix A.4 displays the volumetric budget results for both models. A key difference between both models is the predicted inflow of water into the mine. The predicted inflow rates into the mine pit as a result of dewatering were noticeably lower in the open-source model compared to the site-specific field data model. The site-specific data model has an inflow of water of 24.01 m^3/hr, whereas the open-source data model has an inflow of water of 10.8 m^3/hr.

According to the Wladis (2008), the deep part of the mine contributes approximately 25 m^3/hr, so the site-specific data model predicts a close match to the actual inflow. This suggests that the open-source model may not accurately represent the site-specific conditions. Further investigation and calibration of the open-source model may be necessary to improve its accuracy in predicting water inflow rates.

Field topography is complex, making it quite difficult to assign actual recharge. Furthermore, the geological map shows the presence of folds, structural cracks, and deformation lines around this mine. It is difficult to model these components, but by taking them into account, the accuracy of the model can be increased. Additionally, based on Wladis (2008), there are many shafts around the mine that can change the geology significantly. Implementing the shafts is beyond the scope of this study. In future research, it is crucial to incorporate these geological and structural features into the model to ensure a more accurate and reliable prediction of the mine's performance.

Figure 5-1 and Figure 5-2 show the water head and dewatering impact over a long steady period of time in the open-source data model and site-specific data model due to the construction of mine. Both models exhibit a similar pattern in the radius of influence (ROI) around the mine. According to ROI for both models, this mine will have an impact on the greater region. This information can be used to assess the potential impacts on nearby lakes and design appropriate mitigation measures to protect these water resources from contaminants that are released during mining activity.

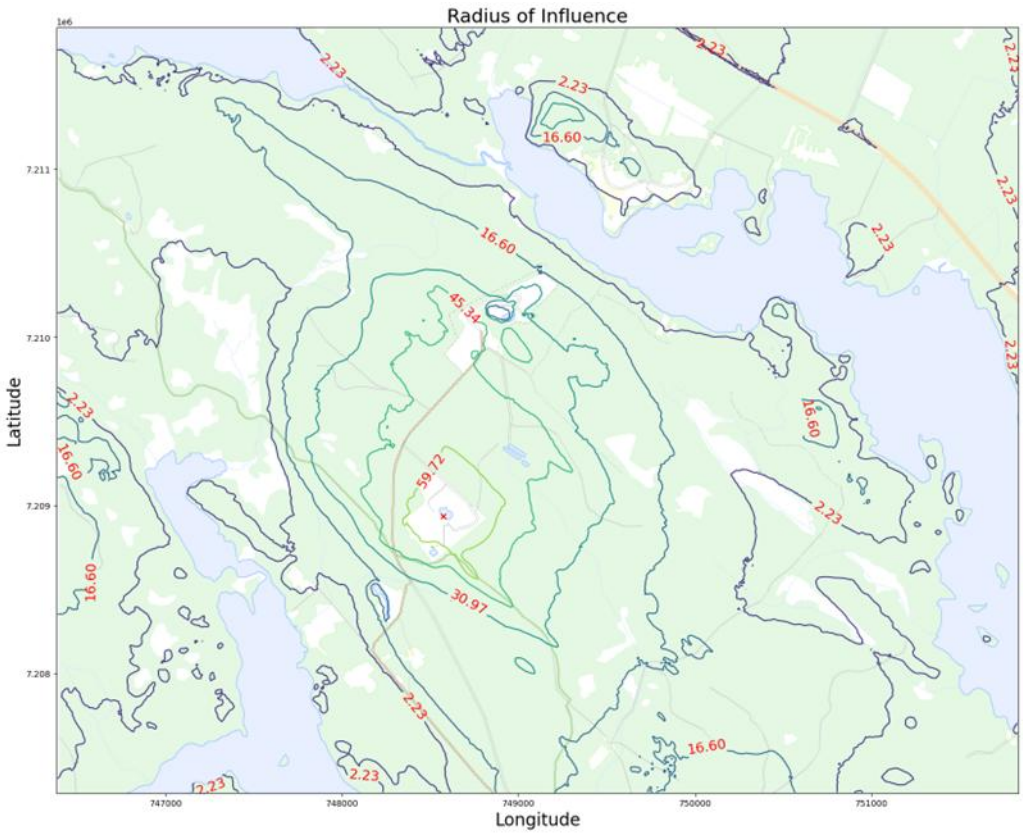

Figure 5-1. Radius of influence of site-specific data model.

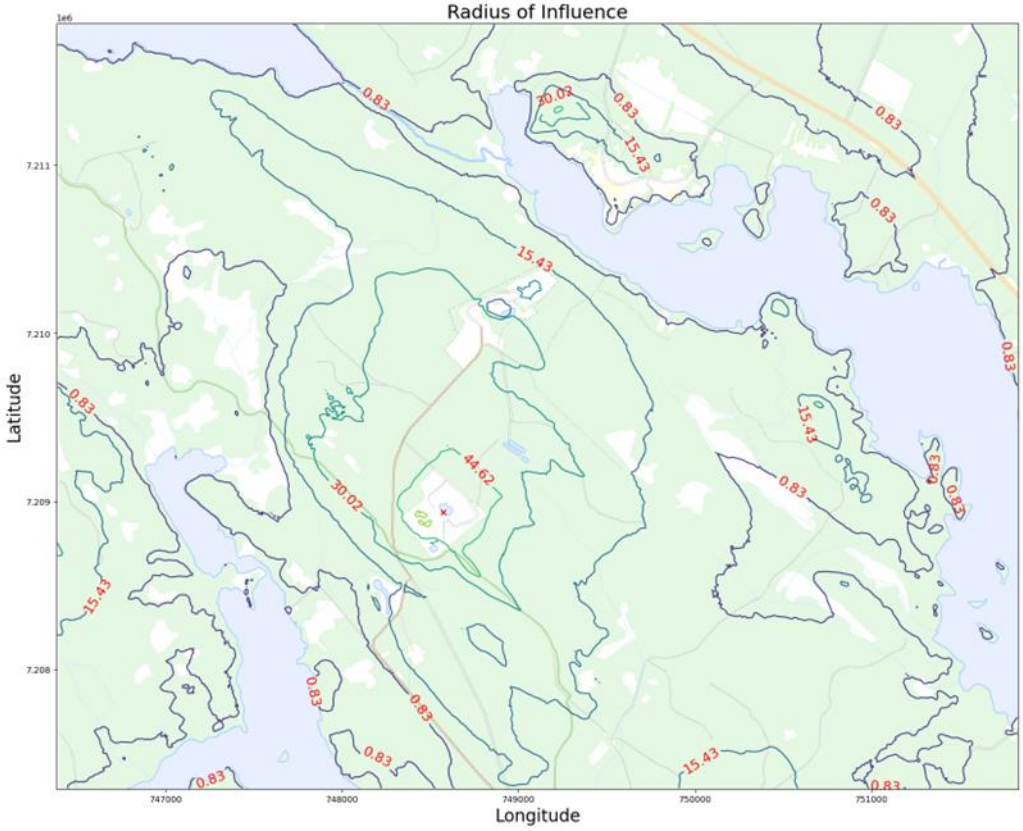

Figure 5-2. Radius of influence of open-source data model.

The predicted hydraulic gradient and flow direction maps for each layer for the open-source data model are shown in Figure 5-3 Arrows illustrate the magnitude and orientation of simulated hydraulic gradients. These maps provide valuable information on the direction and intensity of groundwater flow within the desired location of the mine. Additionally, the predicted hydraulic gradients help in understanding how water moves through different layers of the stratigraphy, aiding in the assessment of potential water inflow into the mine.

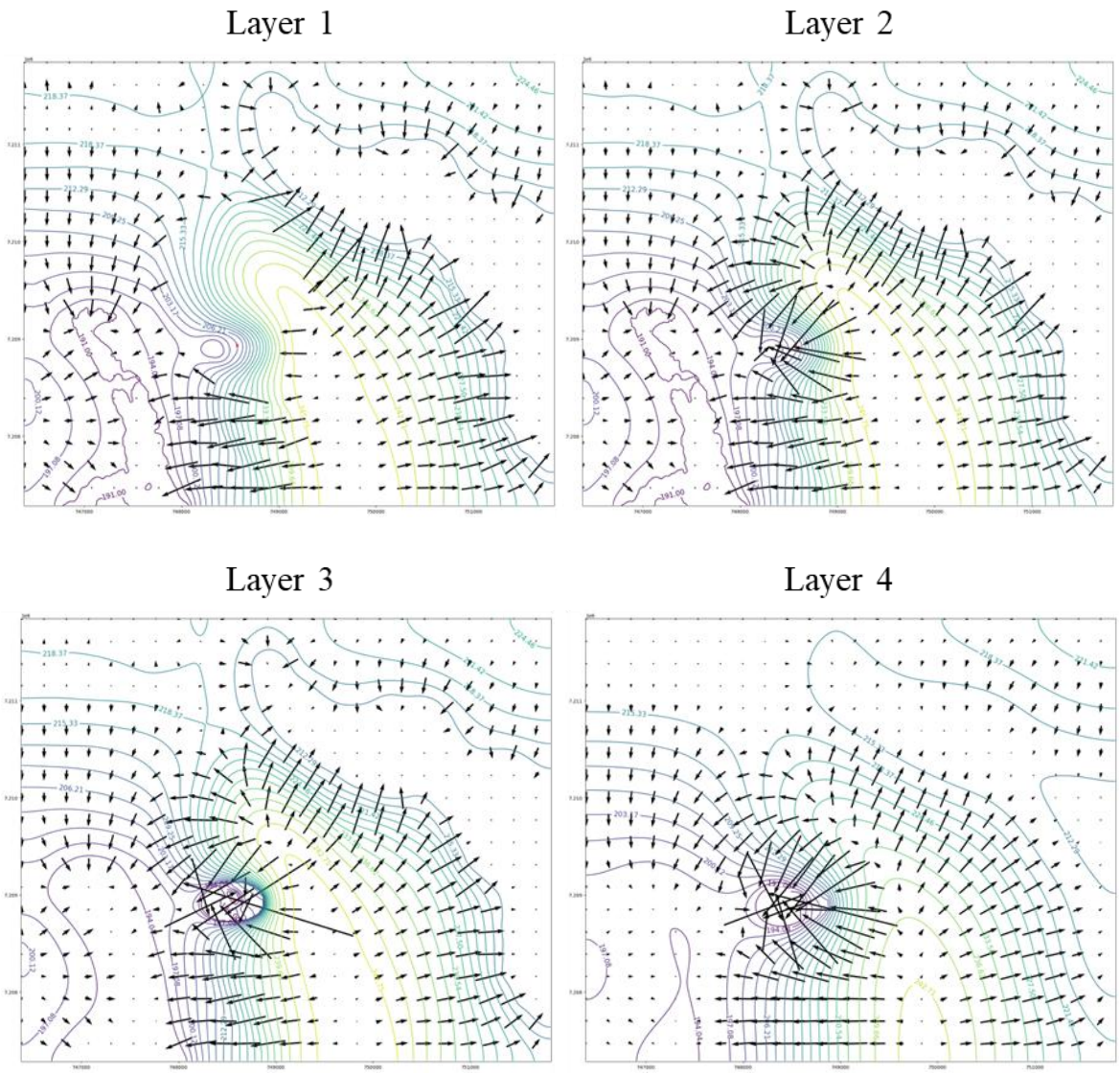

Figure 5-3. Flow direction maps for each layer for the open-source data model.

The predicted hydraulic gradient and flow direction maps for each layer for the site-specific data model are shown in Figure 5-4. There is one more significant resemblance between open-source data and site-specific data models. Similar patterns of hydraulic gradients and highest water levels within every layer are showed by both models. In particular, the general orientation and magnitude of flow gradients generated from model outputs are somewhat consistent between both models at similar depths. Despite variations in input data sources and

calibration aims, the convergence on intra-layer flow patterns and water level distributions indicates that both models are capturing essential elements of the subsurface hydrogeology.

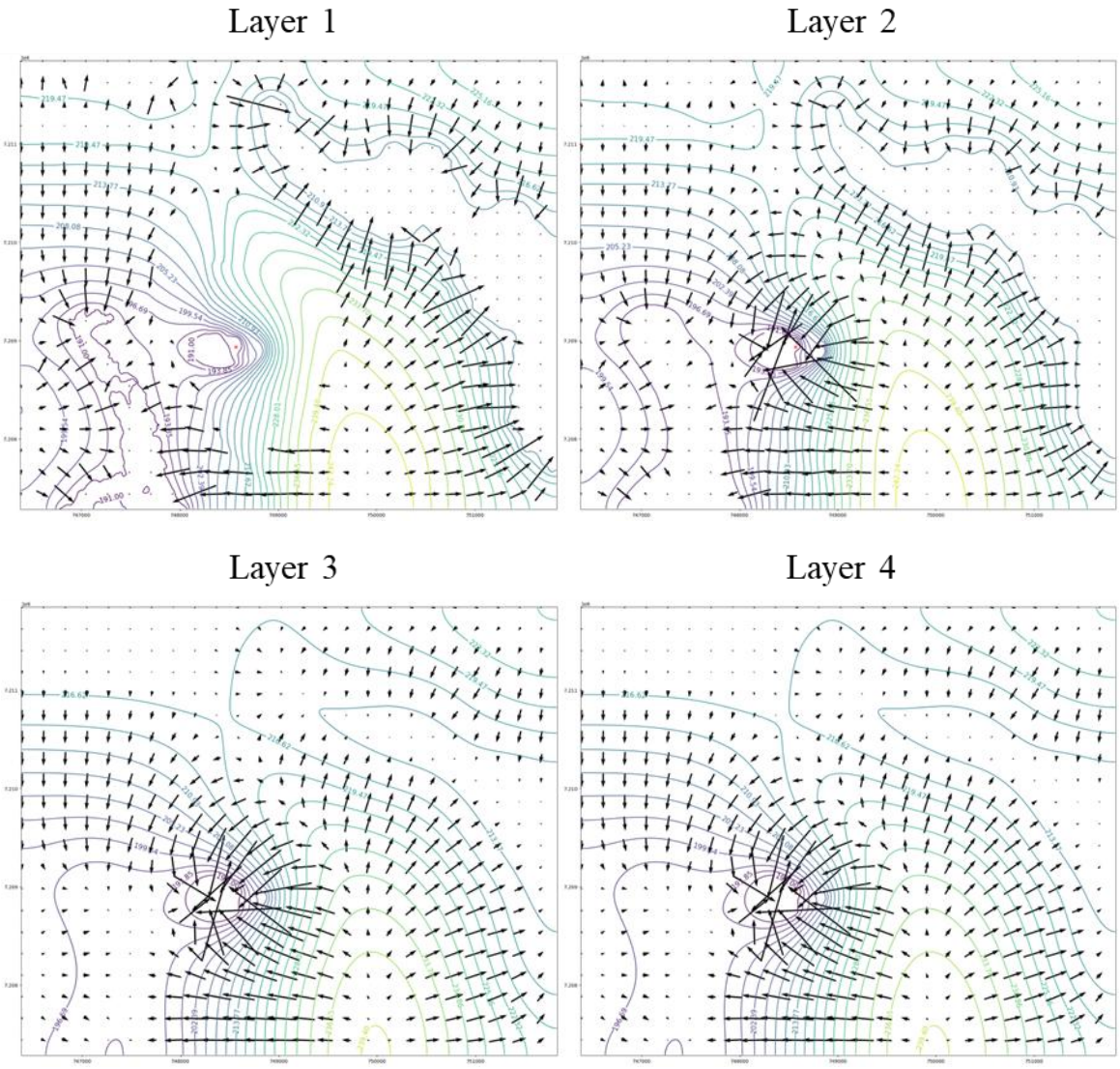

Figure 5-4. Flow direction maps for each layer for the site-specific data model.

These maps are crucial for mine planning and design as they provide valuable information on the potential pathways for water movement within the mine site. gain insights into the overall behavior of water flow in the Kankberg mining project. This can help them understand how water interacts with the fractured rock system and assess potential environmental impacts on a larger scale. Furthermore, these maps can also be used to optimize the placement of dewatering systems and ensure efficient groundwater management during mining operations.

6

Discussion

The results of the study provide significant insights into the groundwater flow system at the Kankberg mine site. This study set out to identify a more affordable way to learn about the site than the more costly site testing method. The process involves comparing the hydrogeological results of numerical modelling using open-source data compared to using site-specific data. The objective is to evaluate the reliability and accuracy of using readily available information for modeling groundwater flow in mining environments. This comparison allowed us to evaluate the applicability of these modeling strategies in similar working environments and potentially enhance their effectiveness for future studies or assessments. It might be less expensive than collecting data at each location specifically. Site-specific data collection involves lengthy, expensive field investigations that require a lot of time and resources.

Open-source data, such as satellite imagery and publicly available reports, can play a valuable role in the early stages of project assessment and planning. It can also provide a broad overview of the project area and help identify potential risks or constraints. However, it is important to note that open-source data may lack specific details or accuracy needed for precise analysis or may not be up to date, which can impact the reliability of the models or predictions. Additionally, relying solely on open-source data may limit the ability to capture site-specific nuances or unique characteristics that can only be obtained through customized field data collection. Customized field data collection allows for ground truthing and validation of open-source information, ensuring that the project's impact assessment is based on reliable and up-to-date data. Therefore, a balanced approach that combines both open-source data and customized field data can provide more robust and comprehensive results for complex projects that have significant infrastructure or environmental impacts. This combination of open source and customized field data enhances the credibility and effectiveness of project planning and decision-making processes.

For the initial modeling, open-source data such as precipitation data and hydraulic conductivity were sourced from the SGU website, which provided reasonable results for groundwater levels and flow direction. Utilizing open-source data has several advantages, such as lower upfront costs, accessibility for studies conducted remotely, and inclusion of larger regional contexts that may be missed in field testing. This suggests that while complex, site-scale applications involving infrastructure or ecological effects may require the collection of customized field data, early modeling or smaller-scale projects with less predictive requirements may benefit from the use of open-source data.

Open-source data can be used for less sensitive projects where a higher level of accuracy is not required. Additionally, the open-source data model may be more cost-effective and readily available, making it a viable option for certain scenarios, like small-scale mining projects and non-critical landslide areas. However, for scenarios that require precise and reliable predictions, such as urban water supply projects or climate-resilient infrastructure, the field-specific data model is recommended to ensure the highest level of accuracy.

The conceptual model oversimplified the complex subsurface conditions by considering each hydrostratigraphic layer as homogeneous and isotropic. However, in reality, there are

different types of bedrock present in the area, and modeling how their permeability will affect groundwater movement is a challenging task. This oversimplification may have led to underestimations or overestimations of hydraulic conductivity values in certain areas. Addressing this discrepancy requires careful interpretation of geological data and a thorough understanding of the structural geology of the area.

Additionally, incorporating faults and structural lines into the model can significantly improve the accuracy of groundwater flow predictions, allowing for more effective and sustainable mining practices. The lack of detailed structural geological data limited the ability to accurately identify and characterize potential preferential flow paths within the aquifer system. Further research and data collection on the structural geology of the study area would greatly enhance the accuracy and reliability of future hydraulic conductivity estimates.

The groundwater drawdown is dependent on both the quantity of water-bearing fractures and their hydraulic properties, which are somewhat interconnected. In practice, permeability, the presence of cracks, and weak zones in the bedrock are important factors that contribute the most to lowering the groundwater table. The absence of this information may contribute to an increase in error.

According to the borehole data from Wladis (2008), rock typically exhibits large natural variations in hydraulic conductivity. The range of variation reaches several orders of magnitude over short distances and in the same depth, making it difficult to establish that greatly affects the groundwater flow in rocks.

During the calibration of open-source data model, an interesting phenomenon was observed regarding the connection between expected groundwater surface elevations and mine inflow rates. The proposed mine pit's inflow was found to be significantly lower when transmissivity and recharge parameters were adjusted to simulate a groundwater surface gradient that resembled the topography of the location. Conversely, setting up the models primarily to achieve inflow quantity similar to what was reported by Wladis (2008) made it challenging to replicate the groundwater gradient that followed the topography of the site area. Accuracy in one parameter came at the expense of the other when trying to model both parameters effectively. This calibration complexity highlights the difficulties in accurately capturing complexly connected systems.

7

Conclusion & Recommendation

This study aimed to assess the prediction capability of numerical groundwater models constructed from two separate data sources: one built with open-source data and the other with data from specific field investigations. Additionally, it seeks to analyze how Kankberg mining operation impact groundwater reserves. In this final chapter, the key findings from results are summarized in the context of addressing the original aims and objectives. Recommendations are also provided based on lessons learned to guide effective future groundwater modeling studies conducted for mine planning and permitting purposes.

The value of more data in a numerical groundwater model lies in its ability to provide a more comprehensive understanding of the system. By incorporating additional data, such as site-specific test pumping data, the model tends to better capture the intricacies and complexities of the groundwater system.

The results of root mean square error indicate that numerical modeling using site-specific data provides more accurate predictions compared to models constructed solely from open-source data. However, the difference in accuracy is limited with only four observation wells used for the calibration of the model based on site-specific data.

The area of the depletion cone in both models indicates that mining operations at Kankberg site have a significant impact on overall groundwater reserves.

Even though the site's true geology is not well understood, site-specific data model almost accurately estimates the rate of inflow of water into the mine.

The study showed that by conducting more thorough field research and gathering additional structural geology data, the process of defining hydraulic conductivity could be further refined. This would lead to more accurate and reliable estimates, ultimately improving the overall understanding of water inflow into the mine and enhancing future calibration and simulation processes. The results demonstrate the necessity of working on data collection process and offer helpful suggestions on suitable modeling techniques for assessing mining impacts. Additional research might expand the methodology to include other mining situations. In summary, the study addresses a major gap in understanding the data requirements for numerical modeling use in the mining industry. Results from an open-source data model are not too far off from reality. Overall, this research highlights the importance of refining data collection methods and utilizing a combination of data sources for more accurate predictions in the mining sector.

Bibliography

Allen, R.L., Weihed, P., Svensson, S-Å. (1996): Setting of Zn-Cu-Au-Ag massive sulphide deposits in the evolution and facies architecture of a 1.9 Ga marine volcanic arc, Skellefte district, Sweden. Economic Geology 91, p.1022-1053.

Appels, M, W., Chris B., G., Jim E., F., & Jeffrey J., M. (2015). Factors affecting the spatial pattern of bedrock groundwater recharge at the hillslope scale. HYDROLOGICAL PROCESSES, 1. https://doi.org/10.1002/hyp.10481

Anderson, M. P., Woessner, W. W., & Hunt, R. J. (2015). Applied groundwater modeling : simulation of flow and advective transport (2nd edition). Elsevier.

Boliden (2022). Boliden Annual and Sustainability Report 2022. Retrieved from https://vp217.alertir.com/afw/files/press/boliden/202303076693-1.pdf

Bhanja, S., Mukherjee, A., Rangarajan, R., Scanlon, B., Malakar, P., & Verma, S. (2018). Long-term groundwater recharge rates across India by in situ measurements. Hydrology and Earth System Sciences. https://doi.org/10.5194/HESS-23-711-2019.

Boyle, D. P., Gupta, H. V., & Sorooshian, S. (2000). Toward improved calibration of hydrologic models: Combining the strengths of manual and automatic methods. Water Resources Research, 36 (12), 3663–3674. doi: 10.1029/2000WR900207

Chand, R., Chandra, S., Rao, V. A., Singh, V. S., & Jain, S. C. (2004). Estimation of natural recharge and its dependency on sub-surface geoelectric parameters. *Journal of Hydrology*, *299*(1), 67–83. https://doi.org/10.1016/j.jhydrol.2004.04.001

Delottier, H., Pryet, A., & Dupuy, A. (2016). Why Should Practitioners be Concerned about Predictive Uncertainty of Groundwater Management Models?. Water Resources Management, 31, 61-73. https://doi.org/10.1007/s11269-016-1508-2

Doherty, J. (2003, 3). Ground water model calibration using pilot points and regularization. Ground Water, 41 (2), 170–177. doi: 10.1111/j.1745-6584.2003.tb02580.x

Feng, Q., Liu, G., Meng, L., Fu, E., Zhang, H., & Zhang, K. (2008). Land subsidence induced by groundwater extraction and building damage level assessment — a case study of Datun, China. Journal of China University of Mining and Technology, 18, 556-560. https://doi.org/10.1016/S1006-1266(08)60293-X.

Fetter, C. W. (2014). Applied hydrogeology (4th edition). Edinburgh: Persons new international edition.

Goodarzi, M., Abedi-Koupai, J., Heidarpour, M., & Safavi, H. (2015). Evaluation of the Effects of Climate Change on Groundwater Recharge Using a Hybrid Method. Water Resources Management, 30, 133-148. https://doi.org/10.1007/s11269-015-1150-4.

Hssaisoune, M., Bouchaou, L., N'da, B., Malki, M., Abahous, H., & Fryar, A. (2017). Isotopes to assess sustainability of overexploited groundwater in the Souss–Massa system (Morocco). Isotopes in Environmental and Health Studies, 53, 298 - 312. https://doi.org/10.1080/10256016.2016.1254208.

Igboekwe, M., & Ruth, A. (2011). Groundwater Recharge Through Infiltration Process: A Case Study of Umudike, Southeastern Nigeria. Journal of Water Resource and Protection, 3, 295-299. https://doi.org/10.4236/JWARP.2011.35037.

Lee, R., & Biggs, T. (2015). Impacts of land use, climate variability, and management on thermal structure, anoxia, and transparency in hypereutrophic urban water supply reservoirs. Hydrobiologia, 745, 263-284. https://doi.org/10.1007/s10750-014-2112-1.

Lantmäteriet. (2019). Produktbeskrivning GSD-Höjddata, grid 2+. Retrieved from www.lantmateriet.se/geolex,.

Li, H., Cohen, A., Li, Z., & Zhang, M. (2018). The Impacts of Socioeconomic Development on Rural Drinking Water Safety in China: A Provincial-Level Comparative Analysis. Sustainability, 11, 1-12. https://doi.org/10.3390/SU11010085.

Maulé, C., Chanasyk, D., & Muehlenbachs, K. (1994). Isotopic determination of snow-water contribution to soil water and groundwater. Journal of Hydrology, 155, 73-91. https://doi.org/10.1016/0022-1694(94)90159-7.

Panigrahy, B., Singh, P., Tiwari, A., & Kumar, B. (2015). Variation in Groundwater Quality with Seasonal Fluctuation in Jharia Coal Mine Region, Jharkhand, India. Current World Environment, 10, 171-178. https://doi.org/10.12944/CWE.10.1.19.

Praveena, S., Abdullah, M., Aris, A., & Bidin, K. (2010). Groundwater solution techniques: environmental applications.. Journal of Water Resource and Protection, 2, 8-13. https://doi.org/10.4236/JWARP.2010.21002.

Rees, G., Hofgaard, A., Boudreau, S., Cairns, D., Harper, K., Mamet, S., Mathisen, I., Swirad, Z., & Tutubalina, O. (2020). Is subarctic forest advance able to keep pace with climate change?. Global Change Biology, 26, 3965 - 3977. https://doi.org/10.1111/gcb.15113.

SGU. (2023). Hydraulisk konduktivitet i berg. Retrieved from https://apps.sgu.se/kartvisare/kartvisare-hydraulisk-konduktivitet.html

SMHI. (2023). Nederbörd . Retrieved from https://www.smhi.se/data/meteorologi/nederbord

Sun, D., Zhao, C., Wei, H., & Peng, D. (2011). Simulation of the relationship between land use and groundwater level in Tailan River basin, Xinjiang, China. Quaternary International, 244, 254-263. https://doi.org/10.1016/J.QUAINT.2010.08.017.

Sutcliffe. J. V. (2004). Hydrology: A question of balance, IAHS Press.

Voigt, B., & Bradley, J. (2020). *Kankberg – Åkulla Östra*. 54.

Wladis, D. (2008). *Utvärdering av* hydrauliska *tester i bergborrade brunnar och kärnborrhål i Åkulla*. MARK & MILJÖ.

Wanner, P., Aravena, R., Fernandes, J., BenIsrael, M., Haack, E., Tsao, D., Dunfield, K., & Parker, B. (2019). Assessing toluene biodegradation under temporally varying redox conditions in a fractured bedrock aquifer using stable isotope methods.. Water research, 165, 114986 . https://doi.org/10.1016/j.watres.2019.114986.

White, E., Easton, Z., Fuka, D., Collick, A., Adgo, E., McCartney, M., Awulachew, S., Selassie, Y., & Steenhuis, T. (2011). Development and application of a physically based landscape water balance in the SWAT model. Hydrological Processes, 25. https://doi.org/10.1002/hyp.7876.

Winter, T. & Harvey, Judson & Franke, O. & Alley, William. (1998). Ground water and surface water a single resource: U. U.S. Geol. Surv. Circ.. 1139.

Xiao-jun, C. (2012). Research and application on coal-water slurry technology. Guizhou Chemical Industry.

Zarate, E., Hobley, D., MacDonald, A., Swift, R., Chambers, J., Kashaigili, J., Mutayoba, E., Taylor, R., & Cuthbert, M. (2021). The role of superficial geology in controlling groundwater recharge in the weathered crystalline basement of semi-arid Tanzania. Journal of Hydrology: Regional Studies. https://doi.org/10.1016/J.EJRH.2021.100833.

Zecharias, Y., & Brutsaert, W. (1988). Recession characteristics of groundwater outflow and base flow from mountainous watersheds. Water Resources Research, 24, 1651-1658. https://doi.org/10.1029/WR024I010P01651.

A
Appendix

A.1 Kankberg mine x-section

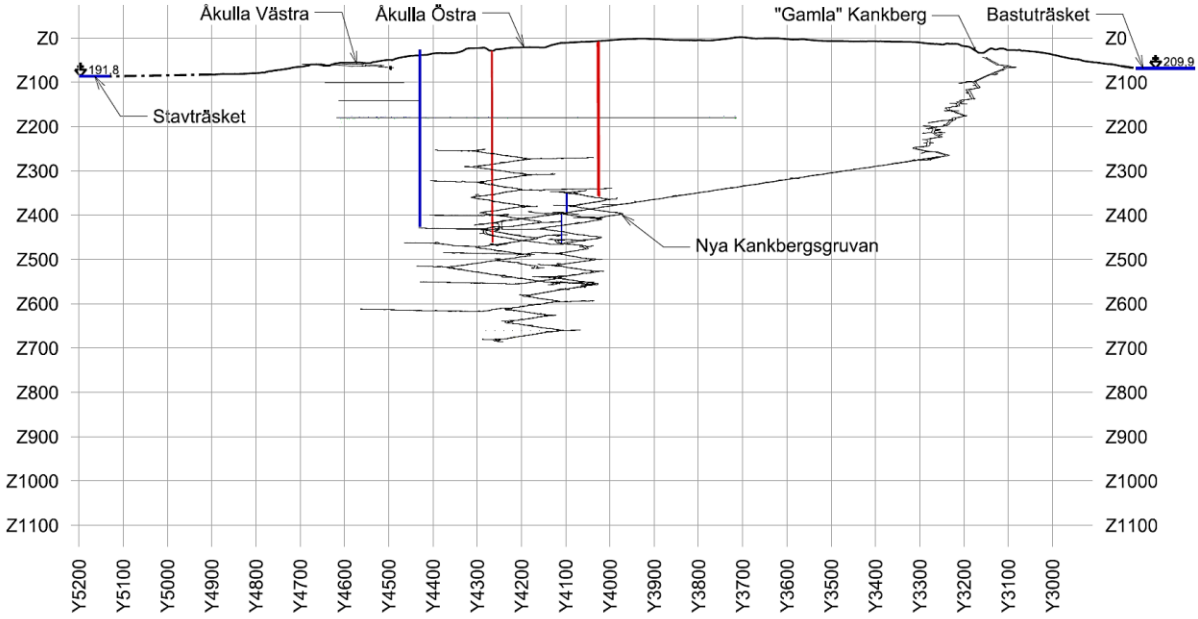

Figure A- A-1. X-section of Kankberg mine.

A.2 Boreholes information

Table A- 1. Borehole information used in site specific data model.

ID	T (m^2/s)	K (m/s)	Depth	Y	X
230100013	7.0E-05	7.2E-07	98	7210200	1712000
905203949*	3.0E-05	5.1E-07	69	7209560	1711007
230100020	5.4E-06	1.0E-07	68	7208900	1708050
905203972*	2.6E-08	6.2E-10	45	7209703	1711336
905203964*	2.1E-07	3.4E-09	69	7209681	1711297
997015110	1.7E-05	2.7E-07	67	7208492	1714171
2301000002	4.3E-06	3.7E-08	115	7206770	1715800
230100038	1.1E-06	7.6E-09	156	7205561	1717397
230100014	2.7E-06	3.3E-08	90	7205500	1717750

230100028	3.3E-06	2.8E-08	123	7201450	1711850
230100004	2.6E-06	1.3E-07	48	7202000	1716750
997081344	4.8E-06	3.0E-08	168	7209630	1703060
997081351	2.0E-05	1.3E-07	160	7209520	1703180
230100009	4.1E-05	1.8E-06	29	7206900	1702900
921011545	5.8E-08	3.0E-10	200	7209493	746016
KA2103B*	7.8E-06	4.0E-08	199	7209148	749058
KA2104B*	2.3E-06	1.2E-08	199	7208764	748789
KA2106B*	1.6E-05	8.6E-08	199	7209056	748443

A.3 Top view of Kankberg mine

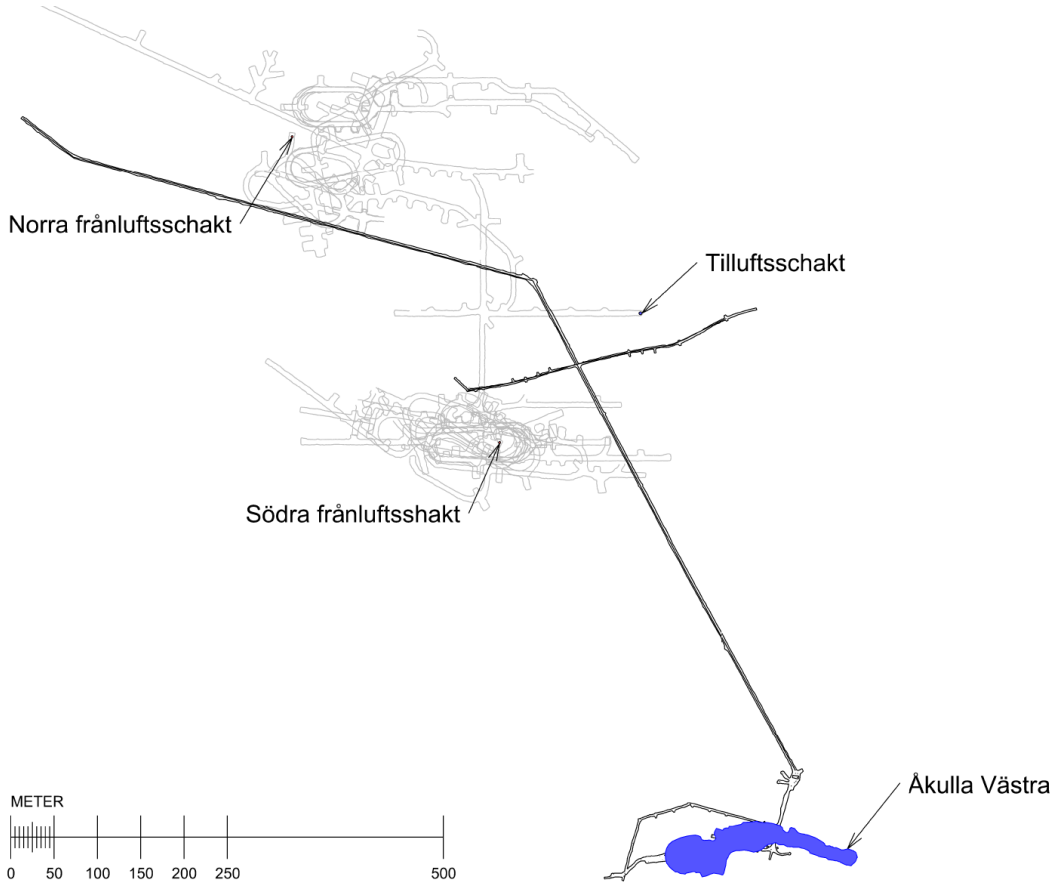

Figure A- A-2. Detailed plan/outline of Kankberg mine.

A.4 Volumetric budget For both model

```
RATES FOR THIS TIME STEP      L**3/T
------------------------

            IN:
            ---
              STORAGE =           0.0000
        CONSTANT HEAD =           0.0000
               DRAINS =           0.0000
             RECHARGE =       3.5389E-02

              TOTAL IN =       3.5389E-02

           OUT:
           ----
              STORAGE =           0.0000
        CONSTANT HEAD =       2.8720E-02
               DRAINS =       6.6702E-03
             RECHARGE =           0.0000

             TOTAL OUT =       3.5390E-02

              IN - OUT =      -4.7684E-07

  PERCENT DISCREPANCY =          -0.00
```

Figure A- A-3. Budget volume diagram of site-specific data model.

```
RATES FOR THIS TIME STEP      L**3/T
-----------------------

            IN:
            ---
              STORAGE =           0.0000
        CONSTANT HEAD =           0.0000
               DRAINS =           0.0000
             RECHARGE =       3.6164E-02

             TOTAL IN =       3.6164E-02

           OUT:
           ----
              STORAGE =           0.0000
        CONSTANT HEAD =       3.3146E-02
               DRAINS =       3.0181E-03
             RECHARGE =           0.0000

            TOTAL OUT =       3.6164E-02

             IN - OUT =      -5.5879E-08

  PERCENT DISCREPANCY =          -0.00
```

Figure A- A-4. Budget volume diagram of open-source data model.

B

Appendix

B.1 Site-Specific Data Model

Required Libraries

In [ ]:
```
import flopy
import os
import flopy.utils.binaryfile as bf
import numpy as np
import matplotlib.pyplot as plt
import rasterio
from rasterio.enums import Resampling
import subprocess
import math
import itertools as it
import platform
from matplotlib.font_manager import FontProperties
from rasterio.features import geometry_mask
from shapely.geometry import shape
from flopy.utils.gridgen import Gridgen
import pandas as pd
from scipy.interpolate import griddata
import geopandas as gpd
```

Input data

In [ ]:
```
rock1 = r'C:\Users\Surface\Downloads\kankberg_model\NewData\Impermeable rocks\impermeable1.shp' #© Lantmäteriet
rock2 = r'C:\Users\Surface\Downloads\kankberg_model\NewData\Impermeable rocks\impermeable2.shp' #© Lantmäteriet
lake0 = r'C:\Users\Surface\Downloads\kankberg_model\NewData\Lakes\Lake0_new.shp' #© Lantmäteriet
lake1= r'C:\Users\Surface\Downloads\kankberg_model\NewData\Lakes\lake1.shp' #© Lantmäteriet
lake2= r'C:\Users\Surface\Downloads\kankberg_model\NewData\Lakes\lake5.shp' #© Lantmäteriet
obser_path = r"C:\Users\Surface\Downloads\kankberg_model\NewData\observation well.csv" #© (Wladis, 2008)
observations = (pd.read_csv(obser_path, delimiter=",").dropna(how='all')).dropna(axis=1, how="all")
```

Create a basic MODFLOW model object

In [ ]:
```
modelname = "Field_Data"
modelpath = "Field_Data_Results"
exe_name = r'C:\Users\Surface\Downloads\kankberg_model\Exe\MODFLOW-NWT_64.exe'
mf = flopy.modflow.Modflow(modelname, exe_name=exe_name, version="mfnwt",model_ws=modelpath)
nwt = flopy.modflow.ModflowNwt(mf ,maxiterout=150,linmeth=2)
```

Open and read raster files

In [ ]:
```
path =r'C:\Users\Surface\Downloads\kankberg_model\NewData\resampled1.tif'  #© Lantmäteriet
dataset = rasterio.open(path)
#dataset.indexes
bedrock_elevation= dataset.read(1)
# Get the geospatial information
transform = dataset.transform
xmin, ymax = transform * (0, 0)
xmax, ymin = transform * (bedrock_elevation.shape[1], bedrock_elevation.shape[0])

# Set axis labels and title
fig, ax = plt.subplots()
im = ax.imshow(bedrock_elevation, extent=[xmin, xmax, ymin, ymax])

# Add a colorbar to show the range of elevations
cbar = plt.colorbar(im , ax=ax)
cbar.ax.set_ylabel('Elevation (m)')

ax.set_xlabel('Longitude')
ax.set_ylabel('Latitude')
ax.set_title('Bedrock Elevation')
plt.show()
np.shape(bedrock_elevation)
```

Spatial discretization

In [ ]:
```
AcuifInf_Bottom = -775 #depth of the model

#Elevation of layers
Layer1 = 0.9 * bedrock_elevation # distractive
Layer2= 0.75 * bedrock_elevation # between
Layer3 = 0.45 * bedrock_elevation #fully solid
Layer_3_4 = -375 # the bottom of the mine
Layer4 = AcuifInf_Bottom #fully solid
```

Column and row number and dimension come from the raster attributes

In [ ]:
```
#Boundaries for Dis = Create discretization object, spatial/temporal discretization
ztop = bedrock_elevation
zbot = [Layer1, Layer2, Layer3,Layer_3_4 , Layer4]
nlay = 5
cellH = 10
vertexCols = np.arange(xmin,xmax+1,cellH)
vertexRows = np.arange(ymax,ymin-1,-cellH)
cellCols = (vertexCols[1:]+vertexCols[:-1])/2
cellRows = (vertexRows[1:]+vertexRows[:-1])/2
ncol = cellCols.shape[0]
nrow = cellRows.shape[0]
delr = cellH
delc = cellH
print('Number of rows: %d and number of cols: %d' % (nrow,ncol))
```

```
Number of rows: 456 and number of cols: 545
```

In [ ]:
```
#Creation of the discretization Funtion

dis = flopy.modflow.ModflowDis(mf, nlay,nrow,ncol,delr=delr,delc=delc,top=ztop,botm=zbot,itmuni=1)
mf.modelgrid.set_coord_info(xoff=xmin, yoff=ymin, angrot=0,epsg=32611)

#dis.plot() #for plotting Dis
```

Model grid representation

In [ ]:
```
# First step is to set up the plot
fig = plt.figure(figsize=(10,12))
ax = fig.add_subplot(1, 1, 1, aspect='equal')

# Next we create an instance of the ModelMap class
modelmap = flopy.plot.PlotMapView(model=mf)

# Then we can use the plot_grid() method to draw the grid
# The return value for this function is a matplotlib LineCollection object,
# which could be manipulated (or used) later if necessary.
linecollection = modelmap.plot_grid(linewidth=0.5, color='royalblue')
```

In [ ]:
```
import matplotlib.colors as mcolors
fig1 = plt.figure(figsize=(20, 6))
ax = fig1.add_subplot(1, 1, 1)
a= np.zeros((nlay, nrow, ncol), dtype=np.int32)
a[0,:,:] = 0
a[1,:,:] = 1
a[2,:,:] = 2
a[3,:,:] = 3
a[4,:,:] = 4
custom_colors = ['yellow', 'green', 'orange', 'brown','grey']
cmap = mcolors.LinearSegmentedColormap.from_list('custom_colormap', custom_colors, N=len(custom_colors))
# Next we create an instance of the ModelCrossSection class
modelxsect_row = flopy.plot.PlotCrossSection(model=mf, line={'Row': 200})
modelxsect_row.plot_array(a, cmap=cmap)
# Then we can use the plot_grid() method to draw the grid
linecollection = modelxsect_row.plot_grid(linewidth=0.4, color='k')
t = ax.set_title('Row 175 Cross-Section - Model Grid', fontname='Times New Roman', fontsize=16)
```

In [ ]:
```
thickness_layer1 = (bedrock_elevation-Layer1).mean()
thickness_layer2 = (Layer1 - Layer2).mean()
thickness_layer3 = (Layer2 - Layer3).mean()
thickness_layer3_4 = (Layer3 - Layer_3_4).mean()
thickness_layer4 = Layer_3_4-AcuifInf_Bottom
thickness = [thickness_layer1, thickness_layer2, thickness_layer3, thickness_layer3_4 ,thickness_layer4]
thickness
```

Out[ ]:
```
[22.618055, 33.92707, 67.85415, 476.7812, 400]
```

Get the points inside each boundary

In [ ]:
```
def points_inside_polygon (path_name):

    gdf = gpd.read_file(path_name)
    polygon = gdf.unary_union
    mask = geometry_mask([polygon], transform=transform, invert=True, out_shape=bedrock_elevation.shape)
    points_inside_polygon = []
    for i in range(mask.shape[0]):
        for j in range(mask.shape[1]):
            if mask[i, j]:
                lon, lat = transform * (j, i)
                points_inside_polygon.append((lon, lat))
    network = []
    for lon, lat in points_inside_polygon:
        lon_index = int((lon - xmin) / delc)
        lat_index = int((ymax - lat) / delr)
        network.append((lat_index, lon_index))

    return points_inside_polygon, network
```

In [ ]:
```
rock1_points, rock1_network = points_inside_polygon (rock1)
rock2_points, rock2_network = points_inside_polygon (rock2)
lake0_points, lake0_network = points_inside_polygon (lake0)
lake1_points, lake1_network = points_inside_polygon (lake1)
lake2_points, lake2_network = points_inside_polygon (lake2)
```

In [ ]:
```
# Just to test
fig, ax = plt.subplots(figsize=(10, 8))
im = ax.imshow(bedrock_elevation, extent=[xmin, xmax, ymin, ymax], cmap='terrain')
# ax.scatter(*zip(*rock1_points), marker='o', color='green')
# ax.scatter(*zip(*rock2_points), marker='o', color='green')
ax.scatter(*zip(*lake0_points), marker='o', color='blue')
ax.scatter(*zip(*lake1_points), marker='o', color='blue')
ax.scatter(*zip(*lake2_points), marker='o', color='blue')
ax.set_xlabel('Longitude')
ax.set_ylabel('Latitude')
ax.set_title('Bedrock Elevation with Shapefile Overlay')

# Create a colorbar for the elevation data
cbar = plt.colorbar(im, ax=ax)
cbar.ax.set_ylabel('Elevation (m)')

plt.show()
```

Boundary Condition and Starting Head

In [ ]:
```
# Variables for the BAS package
ibound = np.ones((nlay, nrow, ncol), dtype=np.int32)
# #Initial level
strt = np.ones((nlay, nrow, ncol), dtype=np.float32)*(bedrock_elevation-1)


for layer in range(nlay-3):
    for i, j in lake0_network:
        ibound[layer, i, j] = -1
        strt[layer, i, j] = 210


for layer in range(0, nlay-3):
    for i, j in lake1_network:
        ibound[layer, i, j] = -1
        strt[layer, i, j] = 191


for layer in range(nlay-3):
    for i, j in lake2_network:
        ibound[layer, i, j] = -1
        strt[layer, i, j] = 217


bas = flopy.modflow.ModflowBas(mf, ibound=ibound, strt=strt)
```

In [ ]:
```
xmine = 748575
ymine = 7208930

row_mine = int((ymax - ymine) / delr)
col_mine = int((xmine - xmin) / delr)
```

```
fig = plt.figure(figsize=(8, 8))
ax = fig.add_subplot(1, 1, 1, aspect='equal')
modelmap = flopy.plot.PlotMapView(model=mf)


quadmesh = modelmap.plot_ibound(color_noflow='red', color_ch='blue')
linecollection = modelmap.plot_grid(linewidth=0.2, color='royalblue')


ax.scatter(xmin + col_mine * delc, ymax - row_mine * delr, color='green', marker='o', label='Mine Center')
legend_font = FontProperties(family='Times New Roman', style='italic', size=12)
ax.legend(loc='lower right', prop=legend_font)
label_font = {'family': 'Times New Roman', 'size': 12}
ax.set_xlabel('Longitude', fontdict=label_font)
ax.set_ylabel('Latitude', fontdict=label_font)
# Add a legend
ax.legend()
plt.show()
row_mine
```

Calculating Hydraulic Conductivity

In [ ]:
```
Kx = np.ones((nlay, nrow, ncol), dtype=np.float32)


Kx[0,:,:] = 1.80E-06
Kx[1,:,:] = 2.53E-07
Kx[2,:,:] = 9.25E-08
Kx[3,:,:] = 6.93E-08
Kx[4,:,:] = 3.00E-09

upw = flopy.modflow.ModflowUpw(mf, laytyp = [1,1,1,1,0], hk=Kx, vka=Kx, ipakcb=53)
```

Assigning Recharge

In [ ]:
```
#Add the recharge package (RCH) to the MODFLOW model
cons = (1000*31536000)
rech = np.ones((1, nrow, ncol), dtype=np.float32)*70/cons
rech[0, 0:80, 450:545] = 50/cons
rech[0, 100:205, 0:210] = 0/cons
rech[0, 205:310, 0:190] = 0/cons
rech[0, 30:140, 210:400] = 40/cons

rech[0, 205:250, 190:340] = 90/cons
rech[0, 250:330, 190:340] = 90/cons

rech[0, 350:456, 120:270] = 40/cons
rech[0, 370:456, 450:545] = 60/cons

rech_Data = {0: rech}
rch = flopy.modflow.ModflowRch(mf,rech=rech_Data)
rch.plot()
```

Out[ ]:
```
[<Axes: title={'center': 'RECH stress period 1'}>]
```

DRN - Mine as Drain Arae

In [ ]:
```
#Length of the major (a) and minor (b) axis
a = 30 # this is an assumption
b = 20 # this is an assumption

# find the x and y inside and on the ellipse
drData = []
mine = np.zeros(bedrock_elevation.shape, dtype=np.int32)

for x in range(col_mine-a, col_mine+a):
    for y in range(row_mine-b, row_mine+b):
        p = ((math.pow((x-col_mine), 2)/ math.pow(a,2)) + (math.pow((y-row_mine), 2)/ math.pow(b,2)))

        if p <= 1:
            drData.append((x,y))
            mine[y][x] = 1
```

In [ ]:
```
#Add the drain package (DRN) to the MODFLOW model
new_list = []
for lay in range(2, nlay-1):
    for i in range(mine.shape[0]):
        for j in range(mine.shape[1]):
            if mine[i][j] == 1:
                new_list.append([lay,i,j, Layer2[i,j],0.001])
                #new_list.append([lay,i,j,ztop[i,j], 0.01]) # layer, row, column, elevation(float), conductance

mineDrn = {0:new_list}

drn = flopy.modflow.ModflowDrn(mf, stress_period_data=mineDrn)
```

In [ ]:
```
drData2 = [(xmin + elem1*delc, ymax- elem2*delr) for elem1, elem2 in drData]
```

In [ ]:
```
fig, ax = plt.subplots(figsize=(10, 8))

# Plot the model grid cells
ax.imshow(ztop, extent=[xmin, xmax, ymin, ymax], cmap='terrain')

# Plot the center of the mine
ax.scatter(xmin + col_mine* delc, ymax - row_mine  * delr, color='red', marker='x', label='Mine Center')

# Plot the drain cells in the cylinder

ax.scatter(*zip(*drData2), color='blue', marker='o', label='Drain Cell')

# Set labels and title
ax.set_xlabel('Longitude')
ax.set_ylabel('Latitude')
ax.set_title('Mine / Drain Cells')

# Add a legend
ax.legend()
# Show the plot
plt.show()
```

In [ ]:
```
# Add OC package to the MODFLOW model
spd = {(0, 0): ['print head', 'print budget', 'print drawdown', 'save head', 'save budget', 'save drawdown']}
oc = flopy.modflow.ModflowOc(mf, stress_period_data=spd, compact=True)#ihedfm= 1, iddnfm=1
```

Observation Wells

In [ ]:
```
observations["row"] = ((observations["Lat"] - ymin) / delr).astype(int)
observations["column"] = ((observations["Long"] - xmin) / delc).astype(int)
observations["layer"] = 3
observations
```

Out[ ]:

	Well ID	Head	Total Depth	Lat	Long	row	column	layer
0	Well 1	215.23	225.0	7209589.91	748470.02	230	208	3
1	KA2103B	219.90	199.0	7209147.80	749058.32	186	267	3
2	KA2104B	234.75	199.0	7208763.65	748789.06	147	240	3
3	KA2106B	188.73	199.0	7209056.34	748442.99	177	206	3

In [ ]:
```
fig, ax = plt.subplots(figsize=(10, 8))

# Plot the model grid cells
ax.imshow(ztop, extent=[0, ncol, 0, nrow], cmap='terrain')

# Plot the center of the mine
ax.scatter(x=observations["column"], y=observations["row"])

# Set labels and title
ax.set_xlabel('Longitude')
ax.set_ylabel('Latitude')
ax.set_title('Observation well')

# Show the plot
plt.show()
```

In [ ]:
```
observ = []
for i in range(len(observations)):
    layer = observations["layer"][i]
    row = observations["row"][i]
    column = observations["column"][i]
    tds = [[0, observations["Head"][i]]]
    observ.append(flopy.modflow.HeadObservation(mf, layer=layer, row=row, column=column, time_series_data=tds))

hob = flopy.modflow.ModflowHob(mf, iuhobsv=1051, hobdry=-999, obs_data = observ)
```

In [ ]:
```
#Write input files -> write file with extensions
mf.write_input()

#run model -> gives the solution
mf.run_model()
```

```
FloPy is using the following executable to run the model: C:\Users\Surface\Downloads\kankberg_model\Exe\MODFLOW-NWT_64.exe

                                 MODFLOW-NWT-SWR1
    U.S. GEOLOGICAL SURVEY MODULAR FINITE-DIFFERENCE GROUNDWATER-FLOW MODEL
                             WITH NEWTON FORMULATION
                             Version 1.1.4 4/01/2018
                    BASED ON MODFLOW-2005 Version 1.12.0 02/03/2017

                    SWR1 Version 1.04.0 09/15/2016

 Using NAME file: Field_Data.nam
 Run start date and time (yyyy/mm/dd hh:mm:ss): 2024/02/22 18:06:15

 Solving:  Stress period:     1    Time step:     1    Groundwater-Flow Eqn.
 Run end date and time (yyyy/mm/dd hh:mm:ss): 2024/02/22 18:10:07
 Elapsed run time:  3 Minutes, 51.677 Seconds

  Normal termination of simulation
```

Out[ ]:
```
(True, [])
```

Model results post-processing

In [ ]:
```
# Extract the heads
hds = bf.HeadFile(modelpath+'/'+modelname + '.hds')
times = hds.get_times()
head = hds.get_data()
#Extract Drawdown
ddnobj = bf.HeadFile(modelpath+'/'+modelname +'.ddn', text='drawdown', precision='single')
drawdown = ddnobj.get_data()
```

In [ ]:
```
#Reads out the CellBudgetFile (Binary cell-by-cell flow file)
cbb = bf.CellBudgetFile(modelpath+'/'+modelname + ".cbc")
kstpkper_list = cbb.get_kstpkper()
frf = cbb.get_data(text="FLOW RIGHT FACE", kstpkper=(0,0))[0]
fff = cbb.get_data(text="FLOW FRONT FACE", kstpkper=(0,0))[0]
flf = cbb.get_data(text="FLOW LOWER FACE", kstpkper=(0,0))[0]
sqx, sqy, sqz = flopy.utils.postprocessing.get_specific_discharge((frf, fff, flf), mf, head)
```

In [ ]:
```
## Plot the Cross section West-East
fig = plt.figure(figsize=(15,10)) #  since we have 50 and 20
ax = fig.add_subplot(1,1,1)
xsect = flopy.plot.PlotCrossSection(model=mf, line={'COLUMN': 220})

# xsect = flopy.plot.PlotCrossSection(model=mf, line={'ROW': 275})
pc = xsect.plot_array(head, head = head, alpha = 1, vmin =170) #0.4 how thick line
pattches = xsect.plot_ibound(head=head)

wt = xsect.plot_surface(head[0], masked_values=[999.], color='blue', lw=2.5)
linecollection = xsect.plot_grid()
# ax.set_xlim([1800, 2300])
ax.set_ylim([-200, 280])
cb = plt.colorbar(pc, shrink =0.75)
```

In [ ]:
```
fig = plt.figure(figsize=(20, 20))
ax = fig.add_subplot(1, 1, 1, aspect="equal")
modelmap = flopy.plot.PlotMapView(model=mf, layer=i, ax=ax)
lc = modelmap.plot_grid(lw=0.)
ax.scatter(xmin + col_mine* delc, ymax - row_mine  * delr, color='red', marker='x', label='Mine Center')
cs = modelmap.contour_array(drawdown[0], levels=np.linspace(drawdown.min(), drawdown.max(), 8))
plt.clabel(cs, inline=1, fontsize=15, fmt="%1.2f")
plt.show()
```

In [ ]:
```
observations["Simulated Head"] = np.nan


for i in range(len(observations)):
    layer = observations["layer"][i]
    row = observations["row"][i]
    column = observations["column"][i]
    observations.at[i,"Simulated Head"] = head[layer][row][column]

observations
#
```

Out[ ]:

	Well ID	Head	Total Depth	Lat	Long	row	column	layer	Simulated Head
0	Well 1	215.23	225.0	7209589.91	748470.02	230	208	3	210.730225
1	KA2103B	219.90	199.0	7209147.80	749058.32	186	267	3	220.896500
2	KA2104B	234.75	199.0	7208763.65	748789.06	147	240	3	217.777954
3	KA2106B	188.73	199.0	7209056.34	748442.99	177	206	3	216.123260

In [ ]:
```
overflow= head[0,:,:] - bedrock_elevation
overflow.max()
```

Out[ ]:
```
8.914001
```

In [ ]:
```
fig = plt.figure(figsize=(8, 8))
ax = fig.add_subplot(1, 1, 1, aspect='equal')
modelmap = flopy.plot.PlotMapView(model=mf)

linecollection = modelmap.plot_grid(linewidth=0.2, color='black')
overflowed= modelmap.plot_array(overflow)
ax.set_xlabel('Longitude', fontdict=label_font)
ax.set_ylabel('Latitude', fontdict=label_font)
cb = plt.colorbar(overflowed, shrink =0.6)

plt.show()
```

In [ ]:
```
#Make a figure with isochrones and arrows
for i in range(nlay):
    fig = plt.figure(figsize=(20, 20))
    ax = fig.add_subplot(1, 1, 1, aspect="equal")
    modelmap = flopy.plot.PlotMapView(model=mf, layer=i, ax=ax)
    lc = modelmap.plot_grid(lw=0.)
    ax.scatter(xmin + col_mine* delc, ymax - row_mine  * delr, color='red', marker='x', label='Mine Center')
    cs = modelmap.contour_array(head[i], levels=np.linspace(191, head.max(), 20))
    plt.clabel(cs, inline=1, fontsize=15, fmt="%1.2f")
    vectors = modelmap.plot_vector(sqx, sqy, istep=22, jstep=22)
    plt.show()
```

DEPARTMENT OF ARCHITECTURE AND CIVIL ENGINEERING
CHALMERS UNIVERSITY OF TECHNOLOGY
Gothenburg, Sweden 2024
www.chalmers.se

CHALMERS
UNIVERSITY OF TECHNOLOGY